

# Secret Key Generation Via Localization and Mobility

Onur Gungor, Fangzhou Chen, C. Emre Koksal

Department of Electrical and Computer Engineering  
The Ohio State University, Columbus, 43210

**Abstract**—We consider secret key generation by a pair of mobile nodes utilizing observations of their relative locations in the presence of a mobile eavesdropper. In our proposed algorithm, the legitimate node pair makes noisy observations of the relative locations of each other. Based on these observations, the nodes generate secret key bits via information reconciliation, data compression and privacy amplification. We characterize theoretically achievable secret key bit rate in terms of the observation noise variance at the legitimate nodes and the eavesdropper, and show that the performance of our algorithm is comparable to the theoretical bounds. We also test our algorithm in a vehicular setting based on observations made using wireless beacon exchange between the legitimate nodes. To achieve this, we used TelosB wireless radios mounted on the sides of the vehicles, in local roads and freeways. Note that, our approach relies solely on distance reciprocity, thus is not restricted to the use of wireless radios, and can be used with other localization systems (e.g., infrared, ultrasound systems) as well. Overall, this study proves that localization information provides a significant additional resource for secret key generation in mobile networks.

## I. INTRODUCTION

We consider the generation of a common key in a pair of nodes, which move in  $\mathbb{R}^2$  (continuous space) according to a stochastic mobility model. We exploit the reciprocity of the distance between a given pair of locations, view the distance between the legitimate nodes as a common randomness shared by these nodes and utilize it to generate secret key bits using the ideas from source models of secrecy [1].

Unlike the recent plethora of studies (see Section I-A for a brief list of related papers) that focuses on wireless channel reciprocity, a variety of technologies can be used for localization (e.g., ultrasound, infrared, Lidar, Radar, wireless radios), which makes distance reciprocity an *additional resource* for generating secret key bits. Such versatility makes the key generation systems more robust, since different technologies may have different capabilities that wireless RF does not have. For instance, narrow beam width of infrared systems would make them less susceptible to eavesdropping from different angles. Distance reciprocity is highly robust, since the distance measured between any pair of points is identical, regardless of

which point the measurement originates. (e.g., when there is no line-of sight, or when different frequency bands are used each way). Yet, there are various challenges in obtaining reciprocal distance measurements.

To that end, we propose a key generation algorithm, in which the legitimate nodes use a three-stage key generation process: (1) In the first stage, they obtain observations regarding the sequence of distances between them over a period of time as they move in the area. The measurements can be obtained actively through exchange of wireless radio, ultrasound, infrared beacons, or passively by processing existing video images, etc. The beacon signal may contain explicit information such as a time stamp, or the receiving node can extract other means of localization information by analyzing angle of arrival, received signal strength, etc. The nodes perform localization based on the observations of distances, and the statistics of the mobility model, and obtain estimates of their relative locations with respect to each other. (2) In the second stage, the nodes communicate over the public channel to agree on an initial key based on their relative location estimates. Meanwhile, the eavesdropper also obtains some information correlated with the generated key. (3) In the final stage, the legitimate nodes perform universal data compression, and privacy amplification on the initial key to obtain the final key.

The generated final key bits satisfy the following three quality measures: i) reliability, ii) secrecy, and iii) randomness. For reliability, we show that the probability of mismatch between the keys generated by the legitimate nodes decays to 0 with increasing block length. In our attacker model, we consider a single passive eavesdropper, that overhears the exchanged beacons in the first phase, and the public discussion in the third phase, and tries to deduce the generated key based solely on these observations. The attacker can follow various mobility strategies in order to enhance its position statistically to reduce the achievable key rate (possibly to 0). We assume that the attacker does not actively interfere with the observation phase, e.g., by injecting jamming signals, etc., in order not to reveal its presence. For secrecy, we consider Wyner's notion, i.e., the rate at which mutual information on the key leaks to the eavesdropper should be arbitrarily low. For randomness, the generated key bits have to be perfectly compressed, i.e., the entropy should be equal to the number of bits it contains.

Next, we focus on the theoretical limits. Using a source model of secrecy [1], we characterize the achievable secret

The authors are with the Department of Electrical and Computer Engineering, The Ohio State University, Columbus, OH, 43210. This work was in part presented in the Workshop on Physical Layer Security, Globecom 2011.

This work is supported in part by QNRF under grant NPRP 5-559-2-227, and by NSF under grants CNS-1054738, CNS-0831919, CCF-0916664.

The authors would like to thank Prof. Prasun Sinha and his team for sharing the vehicular experiment data.

key bit rate in terms of observation noise parameters at the legitimate nodes and the eavesdropper under two different cases of global location information (GLI): (i) No GLI, in which the nodes do not observe their global locations directly, and (ii) perfect GLI, in which nodes have perfect observation of their global locations, through a GPS device, for example. While the bounds we provide are general for a large set of observation statistics, we further investigate the scenario in which the observation noise is i.i.d. Gaussian for all nodes: (a) First, we study the observation SNR asymptotics, and show a phase-transition phenomenon for the key rate. In particular, we prove that the secret key rate grows unboundedly as the observation noise variance decays, if the eavesdropper does not obtain the angle of arrival observations. Otherwise, it is not possible to increase the secret key rate beyond a certain limit. (b) Then, we provide an opportunistic modification to our algorithm, with the additional assumption that the eavesdropper mobility statistics are available at the legitimate nodes<sup>1</sup>. In this case, legitimate nodes exchange beacons only when they predict a geographic advantage over the eavesdropper. (c) We evaluate the theoretical performance numerically for a simple grid-type model, as a function of beacon power. We compare the bounds with our algorithm and show that our key generation algorithm achieves key rate close to the theoretical lower bounds. We show that with our opportunistic modification, non-zero key rates can be achieved even when the eavesdropper obtains better localization information *on average*. (d) We also evaluate the performance for the case where the eavesdropper strategically changes its location to reduce the secret key rate. Specifically, we consider the strategy where the eavesdropper moves to the middle of its location estimates of the legitimate nodes. We show that with this strategy, the eavesdropper can significantly reduce the secret key rate compared to the case where it follows a random mobility pattern.

Finally, we test our algorithm using real experimental measurements taken in a vehicular environment, where two vehicles, equipped with TelosB motes with omnidirectional wireless radios, cruise in local streets and freeways. We show that our algorithm achieves non-zero secret key rates at very low key-mismatch rates even under extremely pessimistic settings, in which the attacker makes observations in the immediate vicinity of one of the legitimate nodes throughout the process and without any a prior statistical model at the nodes on the mobility patterns. We also show that the generated key passes all the randomness tests in the NIST test suite [27].

In summary, we show that relative localization information can be used as an additional resource for secret key generation. To the best of our knowledge, this is the first work that provides both theoretical and practical analysis on secret key generation via localization.

#### A. Related Work

Generation of secret key from relative localization information can be categorized under source model of information theoretic secrecy, which studies generation of secret key bits

from common randomness observed by legitimate nodes. In his seminal paper [1], Maurer showed that, if two nodes observe correlated randomness, then they can agree on a secret key through public discussion. He provided upper and lower bounds on the achievable secret key rates, considering that the nodes have unlimited access to a public channel, accessible by the eavesdropper. Although the upper and lower bounds have been improved later [2], [3], the secret key capacity of the source model in general is still an open problem. Despite this fact, the source model has been utilized in several different settings [4]–[6].

There is a vast amount of literature on localization (see, e.g., [8], [9] for wireless localization, [15] for infrared localization, and [16] for ultrasound localization). There has been some focus on secure localization and position-based cryptography [10]–[13], however, these works either consider key generation in terms of other forms of secrecy (i.e., computational secrecy), or fall short of covering a complete information theoretic analysis.

A similar line of work in wireless network secrecy considers channel identification [14] for secret key generation using wireless radios. Based on the channel reciprocity assumption, nodes at both ends experience the same channel, corrupted by independent noise. Therefore, nodes can use their channel magnitude and phase response observations to generate secret key bits from public discussion. The literature on channel identification based secret key generation is vast. The works [20]–[25] study key generation with on-the-shelf devices, under 802.11 development platform using a two way radio signal exchange on the same frequency. [26], on the other hand, utilizes the fact that fading is highly correlated on locations that are less than a half wavelength apart, instead of exploiting the reciprocity. Therefore, very close nodes can use public radio signals (e.g., FM, TV, WiFi) could be used to generate secret key bits.

Note that, in most of these works, the security analysis is based on the assumption that the channel gains are modeled as random processes, that are independent of the distances between the nodes, and are independent at locations that are more than a few wavelengths apart. While being appropriate for a non line-of-sight and highly dynamic media, these models do not capture wireless propagation in environments where attenuation is a function of the propagation distance. In such environments, an attacker that has some localization capabilities will gain a statistical advantage by estimating the channel gains based on its distance observations. If the key generation process ignores this advantage, part of the key may be recovered by the attacker and thus the key cannot be perfectly secure. For instance, Jana et. al. [21] focuses on a scenario in which secret key bits based on the received signal strength (RSSI), and show that an eavesdropper that knows the location of the legitimate nodes can launch a mobility attack to force the legitimate nodes to generate deterministic key bits, by periodically blocking and un-blocking their line-of-sight. Similarly, if the eavesdropper is close (less than a wavelength) to one of the legitimate nodes, then eavesdropper will obtain correlated information [26] with the initial generated key, which will reduce the key rate (possibly to 0).

<sup>1</sup>Despite the fact that eavesdropper is passive, it is reasonable to assume certain mobility models under specific settings (e.g., vehicular applications).

Our approach of key generation based on locations, on the other hand, does not make such independence assumptions and is thus, *provably secure* against a mobile eavesdropper with localization capability, as we can *explicitly* calculate the equivocation rate. Thus, the insights provided in this paper can also be valuable for the class of studies on key generation based on wireless channel reciprocity, as we show how one should capture a variety of capabilities of the attackers in finding the correct rate for the key and in designing the appropriate mechanisms to generate a truly secret key. Further recall that, our approach is *not restricted* to the use of wireless radios for localization, and can be used other technologies as well. Therefore, our algorithm provides an additional resource for secret key generation.

The rest of this paper is organized as follows. In Section II, we give the system model, and in Section III, we provide our key generation algorithm. In Section IV, we provide general theoretical performance limits of key generation from localization. In Section V, we study the performance limits in detail for the case where the observation noise terms are additive i.i.d. Gaussian, and propose our opportunistic beacon exchange algorithm. In Section VI, we apply our key generation algorithm to a vehicular setting. We conclude in Section VII. To enhance the flow of the paper, several proofs and derivations are collected in Appendix.

A word about notation: We use  $[x]^+ = \max(0, x)$  and  $\|\cdot\|$  denotes the L2-norm. A brief list of variables used in the paper can be found in Table I.

## II. SYSTEM MODEL

TABLE I: List of variables

var.	Description
$n$	number of slots
$T$	number of steps in public discussion
$d_{ij}$	distance between nodes $i$ and $j$
$\mathcal{L} \in \mathbb{R}^2$	the field where nodes are located
$l_j$	2-D location of node $j$
$\phi_{ij}$	angle between nodes $i$ and $j$
$\hat{d}_j, \hat{\phi}_j$	observation of nodes $j \in \{1, 2\}$ of $d_{12}$ and $\phi_j$
$\hat{d}_{je}$	observation of node $e$ of $d_{je}$ and $\phi_{je}$
$o_j$	complete observations of node $j$ based on available GLI
$s$	location triple $[l_1, l_2, l_e]$
$s^\Delta$	quantized version of location triple, $[l_1^\Delta, l_2^\Delta, l_e^\Delta]$
$\Delta$	quantization resolution
$\psi$	uniform $2 - D$ quantization function
$\tilde{s}^\Delta$	$[\tilde{l}_{1,j}^\Delta, \tilde{l}_{2,j}^\Delta, \tilde{l}_{e,j}^\Delta]$
$\tilde{l}_{k,j}^\Delta$	node $j$ 's estimate of $l_k^\Delta$ based on all its information
$\kappa(\cdot, m)$	$m$ -bit Gray coder
$v_j$	obtained binary key at node $j$ before reconciliation
$u_j$	obtained binary key at node $j$ after reconciliation
$q_j$	obtained binary key at node $j$ after universal compression
$k_j$	final key at node $j$ after universal hashing

### A. Mobility Model

We consider a simple network consisting of two mobile legitimate nodes, called user 1 and 2, and a possibly mobile eavesdropper  $e$ . We divide time uniformly into  $n$  discrete slots. Let  $l_j[i] \in \mathcal{L}$  be the random variable that denotes

the coordinates of the location of node  $j \in \{1, 2, e\}$  in slot  $i \in \{1, \dots, n\}$ , where nodes are restricted to the field  $\mathcal{L} \subset \mathbb{R}^2$ . We use the boldface notation  $\mathbf{l}_j = \{l_j[i]\}_{i=1}^n$ , to denote the  $n$ -tuple location vectors for  $j \in \{1, 2, e\}$ . The distance between nodes 1 and 2 in slot  $i$  is  $d_{12}[i] = \|l_1[i] - l_2[i]\|$ . Similarly,  $d_{1e}[i]$  and  $d_{2e}[i]$  denote the sequence of distances between nodes (1,  $e$ ) and nodes (2,  $e$ ) respectively. We use the boldface notation  $\mathbf{d}_{12}, \mathbf{d}_{1e}, \mathbf{d}_{2e}$  for the  $n$ -tuple distance vectors. Note that, in any slot the nodes form a triangle in  $\mathbb{R}^2$ , as depicted in Figure 1, where  $\phi_{12}[i], \phi_{21}[i], \phi_{1e}[i], \phi_{2e}[i]$  denote the angles with respect to some coordinate axis. We

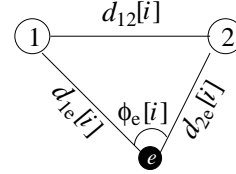


Fig. 1: Legitimate nodes and the eavesdropper form a triangle.

assume that the distances  $d_{12}[i], d_{1e}[i], d_{2e}[i]$  take values in the interval  $[d_{\min}, d_{\max}]$ , since the nodes cannot be closer to each other than  $d_{\min}$  due to physical restrictions, and they cannot be further than  $d_{\max}$  away from each other due to their limited communication range. We assume that the location vectors  $\mathbf{l}_1, \mathbf{l}_2, \mathbf{l}_e$  are ergodic processes. We will use the notation  $s \triangleq [l_1, l_2, l_e]$  to summarize the state variables related to mobility in the system. Note that  $s[i] \in \mathcal{L}^3 = \mathcal{L} \times \mathcal{L} \times \mathcal{L}$  for any  $i$ <sup>2</sup>.

### B. Localization

At each time slot, there is a period in which the legitimate nodes obtain information about their relative position with respect to each other. As discussed in Section I-A, there are various methods to establish the localization information. In this paper, we will not treat these methods separately. We will simply assume that, during measurement period  $i$ , when node 1 transmits a beacon, nodes 2 and  $e$  obtain a noisy observation of  $d_{12}[i]$  and  $d_{1e}[i]$  respectively. Let these observations be  $\hat{d}_2[i]$  and  $\hat{d}_{1e}[i]$ , respectively. Similarly, when node 2 follows up with a beacon, nodes 1 and  $e$  obtain the distance observations  $\hat{d}_1[i]$  and  $\hat{d}_{2e}[i]$ , respectively. The nodes may also independently observe their global positions, e.g., through a GPS device. They may also observe the angle they make with respect to each other, if they are equipped with direction sensitive localizers (e.g., directional antennas in wireless localization). To that end, we consider the following two extreme cases on the global location information (GLI):

- 1) no GLI: We assume that the nodes do not have any knowledge of their global location. However, with the observations of both the beacons, the eavesdropper also obtains a noisy observation,  $\hat{\phi}_e[i]$ , of the angle between the legitimate nodes.
- 2) perfect GLI: We assume that each node has perfect knowledge of its global location, and all nodes have a sense of

<sup>2</sup>It is not necessary to use absolute coordinates for  $\mathbf{l}_1, \mathbf{l}_2, \mathbf{l}_e$ . For example, when global locations are not available at the nodes, we may assume that node 1 is at the origin, i.e.,  $l_1[i] = [0 \ 0]$  for all  $i$

orientation with respect to some coordinate plane as shown in Figure 2. In this case, nodes 1, 2 obtain noisy observations  $\hat{\phi}_1, \hat{\phi}_2$  of the angle  $\phi_{12}$ . Similarly, node  $e$  obtains noisy observation  $\hat{\phi}_{1e}, \hat{\phi}_{2e}$  of the angles  $\phi_{1e}, \phi_{2e}$ .

Let  $o_j[i]$  denote the set of observations of node  $j$  during slot  $i$ , and  $\mathbf{o}_j \triangleq \{o_j[i]\}_{i=1}^n$ . The observations  $\mathbf{o}_j$  for each case is provided in Table II. We emphasize that, the observations in each slot are obtained solely from the beacons exchanged during that particular slot. The nodes' final estimates of the distances depend also on the observations during other slots, due to predictable mobility patterns.

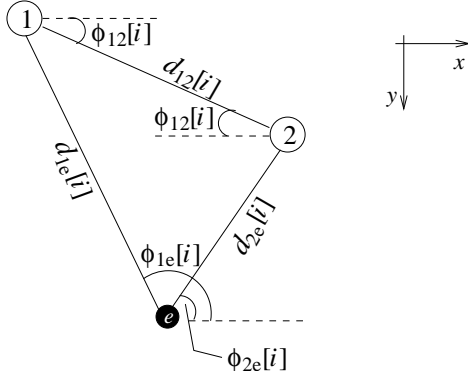


Fig. 2: With GLI, the nodes obtain noisy observations of the relative orientation of each other with respect to the x-axis.

TABLE II: Nodes' Observations

	No GLI	Perfect GLI
$o_1[i]$	$[\hat{d}_1[i]]$	$[\hat{d}_1[i], \hat{\phi}_1[i], l_1[i]]$
$o_2[i]$	$[\hat{d}_2[i]]$	$[\hat{d}_2[i], \hat{\phi}_2[i], l_2[i]]$
$o_e[i]$	$[\hat{d}_{1e}[i], \hat{d}_{2e}[i], \hat{\phi}_e[i]]$	$[\hat{d}_{1e}[i], \hat{d}_{2e}[i], \hat{\phi}_{1e}[i], \hat{\phi}_{2e}[i], l_e[i]]$

### C. Attacker Model

We assume that there exists a passive eavesdropper  $e$ , which does not transmit any beacons. However, node  $e$  can strategically change its location to obtain a geographical advantage against the legitimate nodes. Overall, we consider two strategies:

**Random Mobility:** Eavesdropper moves randomly, without a regard to the location of the legitimate nodes. We will assume that eavesdropper adopts random mobility unless otherwise stated.

**Mobile Man in the Middle:** Node  $e$  controls its mobility, such that it can move accordingly to obtain a geographic advantage compared to legitimate nodes. We consider the strategy where node  $e$  moves to the mid-point of its maximum likelihood estimates of the legitimate nodes' locations. Thus, in slot  $i$ , node  $e$  moves to location

$$\frac{\tilde{l}_{1,e}[i-1] + \tilde{l}_{2,e}[i-1]}{2}, \quad (1)$$

at the beginning of each slot  $i$ , where for  $j \in \{1, 2\}$ ,

$$\tilde{l}_{j,e}[i-1] = \max_{l_j[i] \in \mathcal{L}} \mathbb{P}(l_j[i] | o_e[1], \dots, o_e[i-1])$$

is the maximum likelihood estimate of the location  $l_j[i-1]$  given node  $e$ 's observations until the  $i-1$ 'th slot.

### D. Notion of security

We consider the typical definition of source model of information theoretic secrecy under a passive eavesdropper: We assume that there exists an authenticated error-free public channel, using which the legitimate nodes can communicate to agree on secret keys, based on the observations of the distances and angles ( $\mathbf{o}_1$  and  $\mathbf{o}_2$ ) obtained during beacon exchange. This process, commonly referred to as public discussion [1], is a  $T$  step message exchange protocol, where at any step  $t \in \{1, \dots, T\}$ , node 1 sends message  $C_1[t]$ , and node 2 replies back with message  $C_2[t]$  such that, for  $t > 1$ ,

$$H(C_1[t] | \mathbf{o}_1, \{C_1[i]\}_{i=1}^{t-1}, \{C_2[i]\}_{i=1}^{t-1}) = 0, \quad \text{odd } t \quad (2)$$

$$H(C_2[t] | \mathbf{o}_2, \{C_1[i]\}_{i=1}^t, \{C_2[i]\}_{i=1}^{t-1}) = 0, \quad \text{even } t. \quad (3)$$

At the end of the  $T$  step protocol, node 1 obtains  $\mathbf{k}_1$ , and node 2 obtains  $\mathbf{k}_2$  as the secret key, where

$$H(\mathbf{k}_j | \mathbf{o}_j, \{C_1[t], C_2[t]\}_{t=1}^T) = 0, \quad j \in \{1, 2\}. \quad (4)$$

*Definition 1:* We say that secret key bits are generated (with respect to the described attacker model) at rate  $R$ , if, for all  $\epsilon > 0$  and  $\delta > 0$ , there exists some  $n, T > 0$  such that (2), (3) and (4) are satisfied, and

$$H(\mathbf{k}_j) / n = R, \quad j \in \{1, 2\} \quad (5)$$

$$\mathbb{P}(\mathbf{k}_1 \neq \mathbf{k}_2) \leq \epsilon \quad (6)$$

$$I(\mathbf{k}_j; \mathbf{o}_e, \{C_1[t], C_2[t]\}_{t=1}^T) / n \leq \delta, \quad j \in \{1, 2\}. \quad (7)$$

Here, (5)-(7) correspond to perfect randomness, reliability and security constraints, respectively. The schemes proposed in the source model of secrecy literature typically use a random coding structure, where the messages  $\{C_1[t], C_2[t]\}_{t=1}^T$  are generated by using a binning strategy [1]- [6]. In Section IV, we will make use of these existing results to provide computable theoretical bounds on the achievable key rates.

In practical scenarios, equivocation at  $e$  (7) is difficult to analyze, especially at finite block lengths [31]. To that end, we consider an approximate version of Definition 1 in our key generation algorithm, which is explained in detail in Section III-E.

## III. KEY GENERATION ALGORITHM

In this section, we briefly explain our algorithm in five parts, and provide the complete scheme in Algorithm 1. For guidance, main steps are sketched in Figure 3 for node 1. Prior to first stage, one of the legitimate nodes is appointed to be the *master node*, and is responsible of making several decisions. Without loss of generality, we assume node 1 to be the master node.



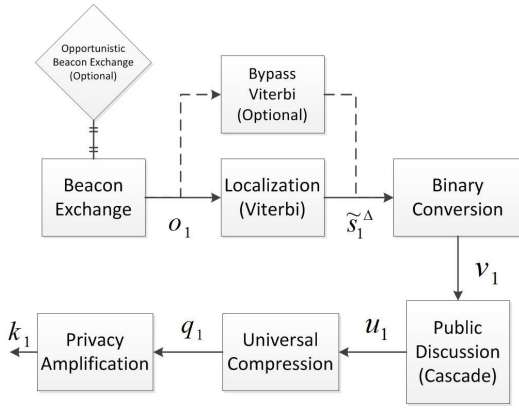


Fig. 3: Key generation algorithm, steps for node 1.

### A. Quantization

First, the nodes quantize the field  $\mathcal{L}$ . Quantization is required for the nodes to efficiently calculate the location estimates and store them in their buffers for use in the subsequent public discussion phase. In our algorithm, we consider the uniform 2-D quantization function  $\psi$ , which is

$$\psi(l, \Delta) \triangleq \arg \min_k \|k - l\|$$

$$\text{subject to: } k = \frac{u\Delta}{\sqrt{2}}, \quad u \in \mathbb{Z}^2.$$

where  $\Delta \triangleq \max_x |x - \psi(x)|$  as the resolution of quantization. Hence, we obtain the quantized field  $\mathcal{L}^\Delta = \{\psi(l, \Delta)\}_{l \in \mathcal{L}}$ , and quantized states  $\mathbf{s}^\Delta \triangleq [l_1^\Delta, l_2^\Delta, l_e^\Delta]$ , where  $\mathbf{s}^\Delta \in \mathcal{S}^\Delta = (\mathcal{L}^\Delta)^3$ .

### B. Beacon Exchange and Localization

In this phase, the legitimate nodes localize to develop the common randomness which serves as the basis for key generation in the following steps. First, beacons are exchanged over  $n$  subsequent slots to form the observation vectors  $\mathbf{o}_1$  and  $\mathbf{o}_2$  as explained in Section II-B. Node  $e$ , on the other hand, overhears the beacons and obtains the observations  $\mathbf{o}_e$ .

Note that each observation vector  $\mathbf{o}_j[i]$  depends solely on the signals exchanged on slot  $i$ , for all  $j \in \{1, 2, e\}$  and  $i \in \{1 \dots n\}$ . In the case where the statistics of the mobility is available at the nodes, each node can find the maximum likelihood estimates  $\tilde{\mathbf{s}}_1^\Delta$  and  $\tilde{\mathbf{s}}_2^\Delta$  of the quantized location triple  $\mathbf{s}^\Delta = [l_1^\Delta, l_2^\Delta, l_e^\Delta]$  where

$$\tilde{\mathbf{s}}_j^\Delta \triangleq \arg \max_{\mathbf{s}^\Delta \in \mathcal{S}^\Delta} \mathbb{P}(\mathbf{s}^\Delta | \mathbf{o}_j), \quad j \in \{1, 2\}. \quad (8)$$

Note that  $\tilde{\mathbf{s}}_j^\Delta = [\tilde{l}_{1,j}^\Delta, \tilde{l}_{2,j}^\Delta, \tilde{l}_{e,j}^\Delta]$ , where  $\tilde{l}_{1,j}^\Delta$  is node  $j$ 's maximum likelihood estimate of node 1 location vector<sup>3</sup>. The terms  $\tilde{\mathbf{s}}_j^\Delta$  are obtained efficiently by using the Viterbi Algorithm as explained in Appendix A-A. Note that:

- For very small  $\Delta$ , it is not computationally feasible to run Viterbi algorithm, since quantized state size  $|\mathcal{S}^\Delta| \nearrow \infty$  as  $\Delta \searrow 0$ .

<sup>3</sup>Since node  $e$  is assumed to be passive and does not transmit any beacons,  $\tilde{l}_{e,j}^\Delta$  depends solely on the eavesdropper mobility statistics at the legitimate nodes. If this information is not available, then it can safely be assumed that  $\tilde{l}_{e,j}^\Delta = \emptyset$ .

- If mobility statistics is not available at the nodes, then ML estimate of the node locations at a given slot depend solely on the observations on the particular slot.

For these cases, we skip Viterbi algorithm. For perfect GLI, instead of (8), we use

$$\tilde{l}_{2,1}^\Delta[i] = l_1^\Delta[i] + \hat{d}_1[i] \angle \phi_1[i], \quad \forall i$$

$$\tilde{l}_{1,2}^\Delta[i] = l_2^\Delta[i] + \hat{d}_2[i] \angle \phi_2[i], \quad \forall i$$

Note that in perfect GLI, each node knows its global location:  $l_j^\Delta[i] = \tilde{l}_{j,j}^\Delta[i]$  for  $j \in \{1, 2\}$ . On the other hand, for no GLI, the angle and global location observations are not available at the legitimate nodes. Hence, the nodes do not have any useful information about each other's 2-D location. Therefore, they only use their 1-D distance observations in the following public discussion stage, instead of their 2-D location estimates, i.e., we set  $\tilde{\mathbf{s}}_1^\Delta = \hat{\mathbf{d}}_1$  and  $\tilde{\mathbf{s}}_2^\Delta = \hat{\mathbf{d}}_2$ .

### C. Binary Conversion and Public Discussion

First, each node  $j \in \{1, 2\}$  obtain an initial  $m$  bit binary sequence

$$v_j[i] \triangleq \kappa(\tilde{l}_{1,j}^\Delta[i] - \tilde{l}_{2,j}^\Delta[i], m), \quad (9)$$

where

$$\kappa(\cdot, m) \triangleq (\mathcal{L}^\Delta - \mathcal{L}^\Delta) \rightarrow \{1 \dots 2^m\}$$

is a Gray coder, which maps the 2-D difference of location estimates to  $m$  bit binary sequences. Let  $\mathbf{v}_j = [v_j[1] \dots v_j[n]]$  represent concatenated version of bit sequences, of size  $nm$  bits. Due to the noisy nature of the observations, the bit mismatch rate (BMR) between the sequences  $\mathbf{v}_1$  and  $\mathbf{v}_2$ , denoted as  $\text{BMR}(\mathbf{v}_1, \mathbf{v}_2)$ , can be significant. To correct bit mismatches, nodes 1 and 2 exchange  $T$  binary messages  $(C_1[1], \dots, C_1[T])$  and  $(C_2[1], \dots, C_2[T])$  over the public channel, to agree on almost identical initial keys  $\mathbf{u}_1$  and  $\mathbf{u}_2$ , respectively, such that

$$\text{BMR}(\mathbf{u}_1, \mathbf{u}_2) < \delta \quad (10)$$

where  $\delta > 0$  can be chosen low enough such that the reliability constraint is satisfied. The process is referred to as information reconciliation by public discussion [1]. In our algorithm, we use Cascade reconciliation protocol [28], which is covered in Appendix A-B.

Cascade reconciliation algorithm performs efficiently when BMR of the initial sequences is low enough such that [28]

$$\text{BMR}(\mathbf{v}_1, \mathbf{v}_2) < 0.15. \quad (11)$$

Parameter  $m$  is chosen largest possible such that (11) is satisfied. On the other hand,  $T$  is variable, and depends on bit sequences and intermediate Cascade parameters, explained in Appendix A-B.

#### D. Universal Compression

After public discussion phase, we have satisfied the reliability constraint. However, we have not satisfied the randomness and secrecy constraints yet: Due to predictable mobility patterns of legitimate nodes, it is possible that  $\mathbf{v}_j$ , hence  $\mathbf{u}_j$  may not be perfectly random. Furthermore, the eavesdropper obtains information correlated with  $\mathbf{u}_j$  due to two reasons: The eavesdropper's observations  $\mathbf{o}_e$  are correlated with the legitimate nodes' observations  $\mathbf{o}_1, \mathbf{o}_2$ , the parity bits exchanged during cascade protocol in public discussion phase reveals some information about the keys  $\mathbf{u}_1$  and  $\mathbf{u}_2$  to the eavesdropper. Therefore, in the following two stages, we compress and hash the keys  $\mathbf{u}_1$  and  $\mathbf{u}_2$  to obtain smaller keys that satisfy randomness and secrecy constraints.

Legitimate nodes first compress their key sequences  $\mathbf{u}_1$  and  $\mathbf{u}_2$  using a universal compression function  $H_c(\cdot)$  to obtain

$$\mathbf{q}_j = H_c(\mathbf{u}_j), j \in \{1, 2\} \quad (12)$$

where the bit sequences  $\mathbf{q}_j$  are of size  $nR'$  bits. In our algorithm, we use Deflate/Inflate compression library for function  $H_c(\cdot)$  [29]. Let the compression ratio be denoted by  $\alpha \triangleq \frac{R'}{m}$ .

#### E. Privacy amplification

Legitimate nodes will map their compressed keys  $\mathbf{q}_1$  and  $\mathbf{q}_2$  into shorter sequences,  $\mathbf{k}_1$  and  $\mathbf{k}_2$ , of key bits in such a way that perfect secrecy condition (7) in Definition 1 is satisfied. We use the following universal hash function for privacy amplification. Let  $H_a(x, R)$  denote

$$H_a(x) = \text{LSB}_{nR}(a \cdot x) \quad (13)$$

where  $\text{LSB}_{nR}$  is the least significant  $nR$  bits,  $a$  is an element over the binary Galois field  $\text{GF}(2^{nR'})$  and  $x \in \{0, 1\}^{nR'}$  is interpreted an element of  $\text{GF}(2^{nR'})$  with respect to a fixed basis of the extension field over the prime field  $\text{GF}(2)$ . Consequently,  $\{H_a(x)\}_{a \in \text{GF}(2^{nR'})}$  is a universal class of hash functions [7].

In the privacy amplification stage, node 1 first chooses  $a$  randomly and uniformly over  $\text{GF}(2^{nR'})$ , and broadcasts on the public channel. Then, nodes 1 and 2 apply privacy amplification  $\mathbf{k}_1 = H_a(\mathbf{q}_1, nR)$ , and  $\mathbf{k}_2 = H_a(\mathbf{q}_2, nR)$ , respectively.

*Choice of rate  $R$ :* Due to the imperfections associated with quantization and cascade reconciliation protocol, rate  $R$  cannot be chosen to be the theoretical secret key capacity, which is studied in the following section. To satisfy the perfect secrecy condition (7), it suffices to choose rate  $R$  as  $R < R^*$ , where  $R^*$  is the equivocation rate at node  $e$  [7], [18]

$$R^* = \frac{1}{n} H(\mathbf{q}_1 | \mathbf{o}_e, \{C_1[t], C_2[t]\}_{t=1}^T) \quad (14)$$

However, calculation of (14) may be computationally infeasible, as discussed in [31]. In Appendix A-C, we approximate  $R^*$  to obtain

$$\tilde{R}^* = \alpha \left( -\text{BMR}_e \log(\text{BMR}_e) - (1 - \text{BMR}_e) \log(1 - \text{BMR}_e) - \frac{T}{n} \right), \quad (15)$$

which is much easier to evaluate. Here,  $\text{BMR}_e = \frac{\sum_{i=1}^{nm} \mathbf{1}(v_1[i] \neq v_e[i])}{nm}$  is the bit mismatch rate at node  $e$  before public discussion, assuming node  $e$  follows quantization and localization steps as described for legitimate nodes, and obtains initial bit sequence  $\mathbf{v}_e$ .

Note that,  $\text{BMR}_e$  is not perfectly available at the legitimate nodes, since it requires perfect knowledge of  $v_e[i]$ . However, when the mobility, and observation noise statistics of the eavesdropper are available at the master node,  $\text{BMR}_e$  can be approximated using Monte Carlo simulations. Note that this is a reasonable assumption, as security is generally defined with respect to a certain threat model. It even suffices if we do not know the exact statistics, but only know the set of mobility/observation noise statistics that the eavesdropper belongs to (there is a compound nature of the eavesdropper model). For example, we can consider a variety of a class of attackers with distinct mobility patterns. Then we can choose  $\tilde{R}^*$  to secure the keys with respect to the worst possible attacker. While one may think that it is not possible to generate a secret key at a non-zero rate with this conservative approach, our experimental observations presented in Section VI are highly encouraging.

#### IV. THEORETICAL PERFORMANCE LIMITS

In this section, we provide information theoretical bounds on the achievable key rate with perfect reliability. To evaluate these bounds, we assume an idealized system by ignoring the issues associated with quantization, cascade reconciliation protocol, and privacy amplification. Thus, these bounds are valid for *any* key generation scheme that satisfies Definition 1.

*Theorem 1:* A lower bound  $R_L$ , and an upper bound  $R_U$  on the perfectly-reliable key rate achievable through public discussion are

$$R_L = \max \left\{ \lim_{n \rightarrow \infty} \frac{1}{n} [I(\mathbf{o}_1; \mathbf{o}_2) - I(\mathbf{o}_1; \mathbf{o}_e)]^+, \lim_{n \rightarrow \infty} \frac{1}{n} [I(\mathbf{o}_2; \mathbf{o}_1) - I(\mathbf{o}_2; \mathbf{o}_e)]^+ \right\} \quad (16)$$

$$R_U = \lim_{n \rightarrow \infty} \frac{1}{n} \min \{I(\mathbf{o}_1; \mathbf{o}_2), I(\mathbf{o}_1; \mathbf{o}_2 | \mathbf{o}_e)\} \quad (17)$$

respectively, where the observations  $\mathbf{o}_1, \mathbf{o}_2$  and  $\mathbf{o}_e$  are as given in Table II for different possibilities of GLI.

The theorem follows<sup>4</sup> from Theorem 4 in [18], which generalizes Maurer's results on secret key generation through public discussion [1], to non-i.i.d. settings. Note that tighter bounds exist in the literature [2], [3], however we use the above bounds, since they provide much clearer insights into our systems due to their simplicity.

Note that for the special case where the observations  $(o_1[i], o_2[i], o_e[i])$  are i.i.d., we can safely drop the index  $i$ , and denote the joint probability density function of observations as  $f(o_1, o_2, o_e)$ . Therefore, the conditioning on the past and

<sup>4</sup>Theorem 4 of [18] provide general upper and lower bounds including the case where the source processes are not ergodic. In our system model,  $\mathbf{o}_1, \mathbf{o}_2$  and  $\mathbf{o}_e$  are ergodic processes, hence they are information stable, therefore these lower and upper bounds reduce to (16) and (17), respectively [17].

---

**Algorithm 1** Key Generation From Localization
 

---

**Step 0: Quantization**

$$\psi(\cdot, \Delta) : \mathcal{L} \rightarrow \mathcal{L}^\Delta = \{1 \dots M\}^2$$

$$l_j^\Delta[i] \leftarrow \psi(l_j[i])$$

$$s_j^\Delta[i] \leftarrow [l_1^\Delta[i], l_2^\Delta[i], l_e^\Delta[i]]$$

**Step 1: Localization****a: Beacon Exchange**

**for** slot  $i = 1 : n$  **do**

**if** No GLI **then**

$$o_1[i] \leftarrow \hat{d}_1[i]$$

$$o_2[i] \leftarrow \hat{d}_2[i]$$

$$o_e[i] \leftarrow [\hat{d}_{1e}[i], \hat{d}_{2e}[i], \hat{\phi}_e[i]]$$

**else if** Perfect GLI **then**

$$o_1[i] \leftarrow [\hat{d}_1[i], \hat{\phi}_1[i]]$$

$$o_2[i] \leftarrow [\hat{d}_2[i], \hat{\phi}_2[i]]$$

$$o_e[i] \leftarrow [\hat{d}_{1e}[i], \hat{d}_{2e}[i], \hat{\phi}_{1e}[i], \hat{\phi}_{2e}[i]]$$

**end if**

**end for**

**b: Viterbi Algorithm**

node  $j \in \{1, 2\}$

**for** slot  $i = 1 : n$  **do**

**for**  $s^\Delta[i-1] \in \{1 \dots M\}^6$  **do**

**for**  $s^\Delta[i] \in \{1 \dots M\}^6$  **do**

**if**  $f(o_j[1], \dots, o_j[i], \chi_j(s^\Delta[i-1]), s^\Delta[i]) >$

$f(o_j[1], \dots, o_j[i], \chi_j(s^\Delta[i]))$  **then**

$$\chi_j(s^\Delta[i]) \leftarrow (\chi_j(s^\Delta[i-1]), s^\Delta[i])$$

**end if**

**end for**

**end for**

**end for**

$$\tilde{s}_j^\Delta[n] \leftarrow \arg \max_{\chi_j(s^\Delta[n])} f(\chi_j(s^\Delta[n]), \mathbf{o}_j^\Delta)$$

**Step 2: Public Discussion**

**for** slot  $i = 1 : n$  **do**

$$v_j[i] \leftarrow \kappa(\tilde{d}_j^\Delta[i] - \tilde{d}_j^\Delta[i-1])$$

**end for**

$$(\mathbf{u}_1, \mathbf{u}_2, \mathbf{u}_e) \leftarrow \text{CASCADE}(\mathbf{v}_1, \mathbf{v}_2, \mathbf{v}_e)$$

**Step 3: Data Compression**

$$\mathbf{q}_j \leftarrow H_c(\mathbf{u}_j), j \in \{1, 2\}$$

**Step 4: Privacy Amplification**

$$\mathbf{k}_j \leftarrow H_a(\mathbf{q}_j, nR), j \in \{1, 2\}$$


---

future observations in  $R_L$  and  $R_U$  disappear, and the lower and upper bound expressions reduce to

$$R_L = \max \left( [I(o_1; o_2) - I(o_1; o_e)]^+, [I(o_1; o_2) - I(o_2; o_e)]^+ \right) \quad (18)$$

$$R_U = \min(I(o_1; o_2), I(o_1; o_2|o_e)), \quad (19)$$

respectively.

## V. GAUSSIAN OBSERVATIONS

To obtain more insights from theoretical results in Section IV, we focus on the following special case: First, we

assume that the node locations are individually Markov processes such that

$$l_j[i-1] \rightarrow l_j[i] \rightarrow l_j[i+1], j \in \{1, 2, e\},$$

holds for any  $i$ , and their joint probability density function  $f(\mathbf{l}_1, \mathbf{l}_2, \mathbf{l}_e)$  is well defined. Secondly, all observations of distance and angle terms are i.i.d. Gaussian processes. Note that this model is typically used in the literature to characterize observation noise [8], [19]. Using the insights, we develop our opportunistic beacon exchange algorithm, and evaluate the theoretical bounds on a simple 2-D grid.

To that end, for no GLI,  $j \in \{1, 2\}$

$$\hat{d}_j[i] = d_{12}[i] + w_j[i], j \in \{1, 2\} \quad (20)$$

$$\hat{d}_{je}[i] = d_{je}[i] + w_{je}[i], j \in \{1, 2\} \quad (21)$$

$$\hat{\phi}_e[i] = \phi_e[i] + w_{\phi_e}[i], \quad (22)$$

where

$$w_j[i] \sim \mathcal{N} \left( 0, \frac{\gamma(d_{12}[i])\rho_j}{P} \right)$$

$$w_{je}[i] \sim \mathcal{N} \left( 0, \frac{\gamma(d_{je}[i])\rho_e}{P} \right)$$

$$w_{\phi_e}[i] \sim \mathcal{N} \left( 0, \frac{\gamma_\phi(d_{1e}[i], d_{2e}[i])\rho_e}{P} \right)$$

are Gaussian noise processes, where  $P$  is the beacon power. The observation noise variances are increasing functions of the distance, which is modelled by the increasing functions  $\gamma$  for distance observations and  $\gamma_\phi$  for angle observations. The parameter  $\rho_j$ , depends on the capability of the nodes. For instance, in wireless localization,  $\gamma$  and  $\gamma_\phi$  depend on the path loss exponent, and  $\rho$  depend on receiver antenna gain, number of antennas, etc [8], [19].

In perfect GLI, we additionally assume that

$$\hat{\phi}_j[i] = \phi_j[i] + w_{\phi_j}[i], j \in \{1, 2\} \quad (23)$$

$$\hat{\phi}_{je}[i] = \phi_{je}[i] + w_{\phi_{je}}[i], j \in \{1, 2\} \quad (24)$$

$$(25)$$

where<sup>5</sup>

$$w_{\phi_j}[i] \sim \mathcal{N} \left( 0, \frac{\gamma_\phi(d_{12}[i])\rho_j}{P} \right)$$

$$w_{\phi_{je}}[i] \sim \mathcal{N} \left( 0, \frac{\gamma_\phi(d_{je}[i])\rho_e}{P} \right).$$

Clearly, the achievable key rates depend highly on the functions  $\gamma$ ,  $\gamma_\phi$  and  $\rho$ . We will show that, our algorithm achieves non-zero secret key rates even when the eavesdropper is more capable, i.e.,  $\rho_e < \rho_j$ , for  $j \in \{1, 2\}$ . In Section V-C, we evaluate the key rate performance of our algorithm for particular choices of  $\gamma$ ,  $\gamma_\phi$  and  $\rho$ , and compare with the theoretical bounds in Section IV. Yet we emphasize that, our key generation algorithm works in the general case, without the above assumptions on the node locations following a Markov process, and the distance and angle observations being Gaussian, as illustrated in experimental results of Section VI.

<sup>5</sup>For perfect GLI, the angle information is obtained according to a fixed coordinate plane, hence the function  $\gamma_\phi$  has single argument.

Note that, there there may be a bias on these observations due to small scale fading [19]. The effect of biased observations are studied in Appendix D.

### A. Beacon Power Asymptotics

In this part, we analyze the beacon power asymptotics of the system. We show that, if the eavesdropper does not observe the angle<sup>6</sup>, i.e.,  $\hat{\phi}_e = \emptyset$ , then  $R_L$  increases unboundedly with the beacon power  $P$ , which indicates that arbitrarily large secret key rates can be obtained. However, when eavesdropper observes the angle information, then  $R_U$  remains bounded, which indicates that the advantage gained by increasing beacon power is rather limited. To clearly illustrate our insights, we present our results for the no GLI scenario. However, the same conclusion holds for the perfect GLI case as well.

*Theorem 2:* When the eavesdropper obtains angle information, i.e.,  $I(\hat{\phi}_e; \phi_e) > 0$ ,

$$\lim_{P \rightarrow \infty} R_U < \infty. \quad (26)$$

The proof is in Appendix C, where we show that  $\lim_{P \rightarrow \infty} R_U \leq \eta$ , where

$$\begin{aligned} \eta = & \frac{1}{2} \log \left\{ 2\pi \mathbb{E} \left[ \frac{\rho_e}{d_{12}^2} \left( \frac{d_{12}^2 \rho_1}{\rho_e} \gamma(d_{12}) \right. \right. \right. \\ & + 4(d_{1e} + d_{2e})^2 (\sqrt{\gamma(d_{1e})} + \sqrt{\gamma(d_{2e})})^2 \\ & + (4d_{1e}d_{2e} + 64(d_{1e}d_{2e})^2) \gamma_\phi(d_{1e}, d_{2e}) \\ & + 8(d_{1e} + d_{2e})d_{1e}d_{2e} (\sqrt{\gamma(d_{1e})} \\ & + \sqrt{\gamma(d_{2e})}) \sqrt{\gamma_\phi(d_{1e}, d_{2e})} \\ & \left. \left. \left. + 64(d_{1e} + d_{2e})^2 (\gamma(d_{1e}) + \gamma(d_{2e})) \right) \right] \right\} \\ & - \frac{1}{2} \mathbb{E} \left[ \log (2\pi \rho_1 \gamma(d_{12})) \right]. \quad (27) \end{aligned}$$

The parameter  $\eta$  remains finite since the distances take on values in some bounded range  $[d_{\min}, d_{\max}]$  with probability 1. Therefore, the secret key rate remains bounded.

*Theorem 3:* When the eavesdropper does not obtain any angle information, i.e.,  $I(\hat{\phi}_e; \phi_e) = 0$ ,

$$\lim_{P \rightarrow \infty} \frac{R_L}{\frac{1}{2} \log(P)} = \lim_{P \rightarrow \infty} \frac{R_U}{\frac{1}{2} \log(P)} = 1.$$

The proof is provided in Appendix C. Theorem 3 implies that, without the angle observation at the eavesdropper, an arbitrarily large key rate can be achieved with sufficiently large beacon power  $P$ . However, the key rate increases with  $\log(P)$ , which means that increasing the beacon power would provide diminishing returns.

### B. Opportunistic Beacon Exchange Algorithm

Note that observation noise variance terms (20)-(24) are increasing functions of distance. Therefore at certain states  $s[i]$

(e.g., when the eavesdropper is located in between the legitimate nodes), eavesdropper's observation noise variances can be smaller compared to legitimate nodes. Formally speaking, when  $o_1[i]$  and  $o_2[i]$  are both *stochastically degraded* versions of  $o_e[i]$ , i.e., there exists a density function  $f$  such that the condition

$$f(o_j[i]|s[i]) = \int_{x=o_e[i]} f(x|s[i]) \tilde{f}(o_j[i]|x) dx \quad (28)$$

holds for  $j \in \{1, 2\}$ , transmission at slot  $i$  benefits the eavesdropper *more* than it benefits the legitimate nodes. This is due to the fact that, since node locations are not independent across time, the eavesdropper can use the advantage obtained at slot  $i$  to obtain better estimates at slot  $i + 1$ . Therefore, skipping beacon transmission at slots when condition (28) occurs will yield *higher* key rates compared to the case where a beacon is exchanged in every slot. However, it is not feasible for legitimate nodes to verify condition (28) due to two facts:

- 1) It is not computationally feasible to verify condition (28).
- 2) The legitimate nodes do not know each other's exact location, and they do not observe eavesdropper's location at all.

To circumvent these two issues, we consider an approximate version of (28), and consider the likelihood of that new condition, based on the nodes' statistical knowledge of each other's, and the eavesdropper's location.

The details are provided in Algorithm 2. Beacon transmission decisions made by the master node. Let

$$A[i] = \frac{(d_{1e}[i] - d_{2e}[i] \cos(\phi_e[i]))^2 \gamma(d_{1e}[i])}{d_{12}[i]^2} + \frac{(d_{2e}[i] - d_{1e}[i] \cos(\phi_e[i]))^2 \gamma(d_{2e}[i])}{d_{12}[i]^2} \quad (29)$$

$$B[i] = \frac{(d_{1e}[i]d_{2e}[i] \sin(\phi_e[i]))^2 \gamma_\phi(d_{1e}[i], d_{2e}[i])}{d_{12}[i]^2}. \quad (30)$$

where  $\rho_{\max} = \max(\rho_1, \rho_2)$ . The master node decides to skip beacon exchange at slot  $i$  either when the condition

$$\mathbb{P}(\gamma(d_{12}[i])\rho_{\max} < (A[i] + B[i])\rho_e \{o_k[l]\}_{l=i}^{i-1}) < \tau \quad (31)$$

occurs for some predetermined threshold  $\tau$ , and when a beacon exchange has occurred in the previous  $c$  slots, chosen appropriately in order to avoid long droughts leading to the possibility for the nodes to get out of each other's range. The derivation of (31) follows from applying a series of linear approximations to (28), and is provided in Appendix B. Note that the master node do not know the exact values of  $A[i]$ ,  $B[i]$  nor  $d_{12}[i]$ , rather it knows the probability distribution, conditioned on its observations, and statistical knowledge of each other's, and the eavesdropper's location.

If the other legitimate node receives a beacon during slot  $i$ , it replies back with a beacon, otherwise it remains silent. At the end of slot  $i$ , the nodes update their observations, such that if no beacons have been transmitted, then  $o_j[i] = \emptyset$  for  $j \in \{1, 2, e\}$ . The probability in (31) can be efficiently approximated with linear complexity using Forward Algorithm, as provided in Algorithm 2, and illustrated in Appendix B-B.

**Remarks:**

<sup>6</sup>Note that in some cases, the nodes cannot obtain any useful angle information, e.g., in wireless localization, when each node is equipped with a single omnidirectional antenna.



- If the mobility is i.i.d., then no advantage in terms of secret key rate can be obtained by using opportunistic beacon transmission. Still, power would be more efficiently utilized due to less beacon exchanges.
- The algorithm works when the statistical knowledge of eavesdropper mobility is available at the legitimate nodes. Despite the fact that eavesdropper is passive, it is reasonable to assume certain mobility models under specific settings (e.g., vehicular applications).

In Section V-C, we show that our algorithm achieves non-zero secret key rates for some cases that yield zero secrecy rates when a beacon is transmitted every time slot. We also compare our algorithm with the genie aided case, in which a genie knows the exact locations all the nodes in the field, and tells the nodes to skip beacon transmission at slot  $i$  when the condition

$$\gamma(d_{12}[i])\rho_{\max} > (A[i] + B[i])\rho_e$$

is satisfied. The genie aided case provides us an upper bound on the achievable key rate among algorithms that use this condition for beacon transmission decisions.

---

**Algorithm 2** Opportunistic Beacon Exchange

---

**BEACON:**
 $j \leftarrow \text{Master Node}$ 
 $\text{CTR} \leftarrow 0$ 
 $\mathbb{P}(s_1^\Delta[0]) \leftarrow 1/M^6, \forall s_1^\Delta[0] \in \{1 \dots M\}^6$ 
**for** slot  $i = 1 : n$  **do**
 $\zeta \leftarrow 0$ 
**for**  $s^\Delta[i-1] \in \{1 \dots M\}^6$  **do**
**for**  $s^\Delta[i] \in \{1 \dots M\}^6$  **do**
 $x_1 \leftarrow \mathbf{1}(\gamma(d_{12}[i]) > A[i] + B[i]|s^\Delta[i])$ 
 $x_2 \leftarrow f(o_j[1], \dots, o_j[i-1], s^\Delta[i-1])$ 
 $x_3 \leftarrow \mathbb{P}(s^\Delta[i]|s^\Delta[i-1])$ 
 $\zeta \leftarrow \zeta + x_1 x_2 x_3$ 
**end for**
**end for**
**if**  $\zeta < \tau$  **or**  $\text{CTR} \geq c$  **then**

NODE 1 TX BEACON

NODE 2 TX BEACON

 $o_j[i] \leftarrow (\hat{d}_j[i], \Delta)$ 
 $\text{CTR} \leftarrow 0$ 
**else**

NODE 1 SILENT

NODE 2 SILENT

 $o_j[i] \leftarrow \emptyset$ 
 $\text{CTR} \leftarrow \text{CTR} + 1$ 
**end if**
**end for**


---

### C. Numerical Evaluations

We evaluate the key rate performance of our key generation algorithm, and the theoretical bounds in Section IV for Gaussian observations model, using Monte Carlo simulations. We also study the theoretical performance gains of the proposed opportunistic beacon exchange strategy.

*Setup:* We consider a simple  $(M \times M)$  discrete 2-D grid, which simulates a city with  $M$  blocks that covers a square field of area  $A^2$ , such that for any  $j \in \{1, 2, e\}$ ,  $i \in \{1, \dots, n\}$ ,  $l_j[i] = [x \ y] \in \{\frac{A}{M}, \dots, M\frac{A}{M}\} \times \{\frac{A}{M}, \dots, M\frac{A}{M}\}$ . Node mobilities are Markov, and characterized by parameter  $B$ , where

$$\mathbb{P}(l_j[i] = [x \ y] \mid l_j[i-1] = [x' \ y']) = \begin{cases} \frac{1}{(B+1)^2} & \text{if } |x - x'| \leq \frac{AB}{M} \\ & |y - y'| \leq \frac{AB}{M} \\ 0 & \text{otherwise} \end{cases}$$

For no GLI, we choose  $\gamma(d) = 0.1 + d^2$ , and

$$\gamma_\phi(d_{1e}, d_{2e}) = \pi - \frac{\pi}{1.1 + (d_{1e}^2 + d_{2e}^2)},$$

and for perfect GLI, we choose

$$\gamma_\phi(d_{je}) = \pi - \frac{\pi}{1.1 + (d_{je})^2}$$

such that both parameters are strictly increasing functions of the distances.<sup>7</sup> We consider node capability parameters  $\rho_1 = \rho_2 = \rho_e = 1$ , unless stated otherwise. The theoretical key rates in Section IV converge as  $n \rightarrow \infty$ , therefore they are calculated for large enough  $n$ , using the forward algorithm procedure described in Appendix B-B.

*Results:* Due to computational limitations explained in Section III-B, we consider examples in which  $M \leq 11$ , and  $B \leq 3$ . Note that this choice limits the maximum achievable secret key rate<sup>8</sup>. First, we compare the performance of our key generation algorithm with the theoretical capacity bounds provided in Section IV. In Figure 4, we plot the key rates with respect to the *normalized* beacon power  $P/\sigma_0^2$  for  $M = 5$ ,  $A = 5$ , and  $B = 1$ , where  $\sigma_0^2$  denotes the variance of distance observations  $\hat{d}_j[i]$  of legitimate nodes at unit distance. We show that, even in this grid with a small number of possible locations, we can generate reliable key bits comparable with the theoretical bounds. Note that the key rate starts to decrease at a certain beacon power, beyond which the rate of information accumulation at the eavesdropper exceeds that at the legitimate nodes. Also, we emphasize that the lower bound and the upper bound provided in Figure 4 are analytically proven bounds on key capacity, where the lower bound is achieved by using random coding arguments which are not feasible to implement due to computational complexity. Although our algorithm performs worse than the theoretical lower bound, it is implemented using tools that are feasible to use, such as viterbi algorithm, cascade algorithm, etc.

Then, we analyze the effect of the different grid size, field area and GLI on the theoretical key rates. In Figures 5 and 6,

<sup>7</sup>A similar model for distance observation noise is used in [8]. Since  $\phi_e \in [0, \pi]$ , the angle observation error variance cannot diverge with distance, and we upper bounded the variance term by  $\pi/1.1$ . To avoid zero error variances at zero distance, we introduce a 0.1 offset to numerator and denominator of  $\gamma$  and  $\gamma_\phi$ , respectively.

<sup>8</sup>For instance, for the choice of  $B = 1$ , due to the limited mobility of the nodes, there are 13 different possible distance combinations. Consequently, a key rate of  $\log 13$  is an absolute upper bound on the key rate for no GLI even in the case when the eavesdropper does not obtain any distance or angle observation.

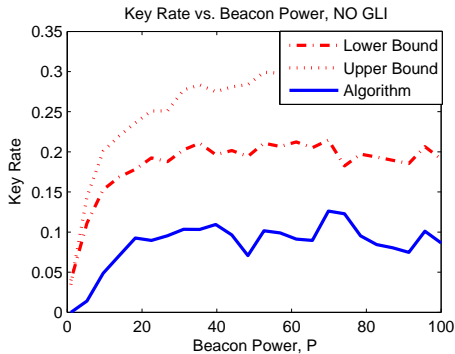


Fig. 4: Comparison of theoretical bounds and key generation algorithm vs normalized beacon power, no GLI

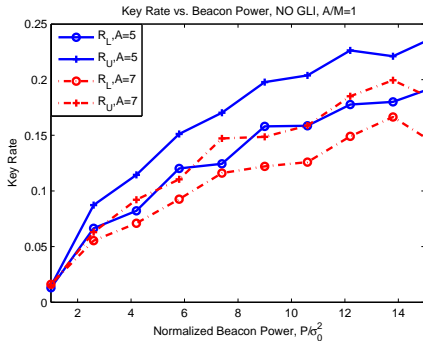


Fig. 5: Bounds for no GLI vs normalized beacon power, for different  $M$ ,  $B = 1$ ,  $A/M = 1$

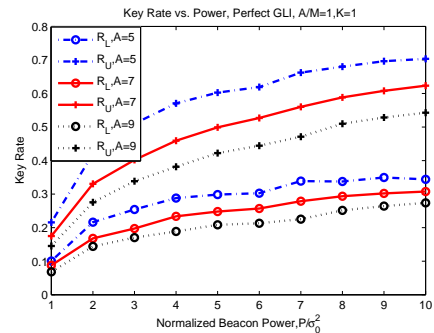


Fig. 6: Bounds for perfect GLI vs normalized beacon power, for different  $M$ ,  $B = 1$ ,  $A/M = 1$

we plot the bounds on the achievable key rate with respect to the normalized beacon power  $P/\sigma_0^2$  for different grid size  $M$  for no GLI and perfect GLI cases, respectively. We assumed a constant ratio of field size and grid size,  $A/M = 1$ , and considered  $B = 1$ . We can see that, there is a diminishing return on the increased power levels for the achievable key rate. Furthermore, we can see that increasing the field area  $A^2$  has a negative impact on the key rate despite the increase in  $M$ , which is due to the fact that the common information of the legitimate nodes decreases as a result of increase in their observation error variance. Next, in Figures 7 and 8, we plot the bounds with respect to beacon power  $P$ , for different step size  $B = 1$  for no GLI and perfect GLI cases, respectively. We assumed  $M = 5$  for the no GLI case, and  $M = 7$  for perfect GLI case, and in both cases, the ratio of field size and grid size is constant, such that  $A/M = 1$ . We can clearly see the positive effect of the increased step size on the secret key rate. This is due to the increase in different distance combinations that are possible. Next, for no GLI, we evaluate

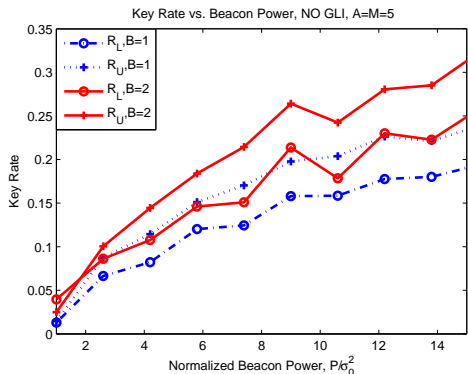


Fig. 7: Upper and lower bounds for no GLI vs normalized beacon power  $P/\sigma_0^2$ ,  $M = A = 5$ , for different  $B$

the theoretical performance of opportunistic beacon exchange scheme as well as the impact of the eavesdropper mobility scheme, both described in Section III. First, we show that, even under a pessimistic scenario for the legitimate nodes, non-zero secret key rates can be achieved by our opportunistic scheme, which would not be possible with the non-opportunistic case:

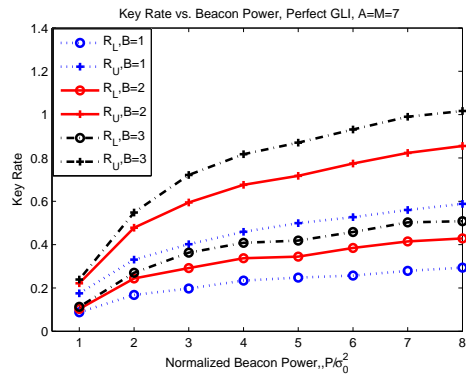


Fig. 8: Upper and lower bounds for perfect GLI vs normalized beacon power  $P/\sigma_0^2$ ,  $M = A = 7$ , for different  $B$

We assume that node  $e$  is more capable such that  $\rho_1 = \rho_2 = 1$  and  $\rho_e = 0.6$ , which can model the case where node  $e$  is equipped with more antennas compared to the legitimate nodes. Furthermore, node  $e$  stays fixed at the center of the  $M \times M$  grid, for  $M = 7$  and  $A = 5$  and  $B = 1$ . Since the observation noise variance is an increasing function of the node distances, this also gives node  $e$  a geographic advantage over the legitimate nodes 1 and 2. We can see from Figure 9 that secret key rate decays to 0 with the non-opportunistic scheme. On the other hand, non-zero secret key rates can be achieved with our opportunistic strategy outlined in Section III, for parameters  $\tau = 0.5$  and  $c = 4$ . On the same figure, we also plot the achievable key rates for the genie-aided scheme, which has the reach to the perfect side information on whether the legitimate nodes have a geographical advantage or not at any given point in time. With such side information, the key rate is roughly doubled compared to our opportunistic scheme. Note that our algorithm obtains information on the presence of a geographical advantage, based solely on the beacon observations. One of the issues is that, when the two legitimate nodes skip beacon transmissions, their information on each other's location becomes more degraded, hence they cannot predict whether they still keep the geographic advantage compared to the eavesdropper. Despite the fact that our algorithm skips on the average 69% of the beacon transmissions due to a predicted

geographic disadvantage, it is remarkable that roughly half the key rate is achievable with our scheme compared to the case with the genie-aided perfect side information.

Finally, we analyze the effect of eavesdropper mobility on the achievable key rate. In Figure 10, for  $M = 7$ ,  $A = 5$  and  $B = 1$ , we plot the secret key rate bounds versus beacon power for the cases where the eavesdropper i) follows the random mobility pattern described in the setup with parameter  $B = 1$ , ii) stays at the origin, and iii) follows the man in the middle strategy described in Section II-C, i.e., moves to the mid point of its location estimates of nodes 1 and 2. We can see that, compared to following a random mobility pattern, the eavesdropper can reduce the achievable secret key rate significantly by following this strategy. Also, the eavesdropper can significantly reduce the key rate by simply staying static at a certain favorable location, rather than moving randomly. Note that, in practice this may not be feasible for the eavesdropper, since, by staying put, it will lose connection completely with the legitimate nodes in a large region.

## VI. EXPERIMENTAL EVALUATIONS

Finally, we test our key generation algorithm in a vehicular setting with wireless radios. We used two vehicles, A and B, each equipped with TelosB notes. Omnidirectional antennas placed above wheels of each vehicle, as shown in Figure 12, are connected to TelosB notes. Beacons are transmitted from antennas periodically, and RSSI (Received Signal Strength Indicator) measurements are collected for transmitter-receiver antenna pairs.

We use the rear left antenna of vehicle A and the front left antenna of vehicle B as nodes 1 and 2, respectively. Similarly, we take the measurements from the rear right antenna of vehicle A to be the eavesdropper observations. Note that, in this case the distance between node 1 and node  $e$  is fixed and we assume that this distance  $d_{1e}$ , and the angle  $\phi_e$  are known perfectly by node  $e$ . We also assume that nodes 1 and 2 do not have the mobility statistics, or their individual global locations (hence no GLI). Thus, the scenario we are trying to emulate with this experiment is one, that is extremely favorable for the eavesdropper (an attacker that collects observations directly from one of the legitimate vehicles). Our main objective here is to illustrate that, even in such highly pessimistic cases, it is possible to generate secret keys at a non-zero rate.

The data is collected from vehicles driven in (i) local and (ii) freeway roads over a period around 30 minutes, where beacon exchange occurs roughly every 2 seconds. Here, we go over the details of our key generation algorithm for data observed as the vehicles cruise on a highway, and consider the first  $n = 1000$  slots. We use a path-loss model<sup>9</sup> to obtain distance observations from beacon RSSI [30],

$$\tilde{d}_j = -22 \log_{10}(\text{RSSI}_j) - 44.8$$

where  $\text{RSSI}_j$  is associated with node  $j$  and the unit is dBm, and  $\tilde{d}_j$  is the distance measurement in meters. The distance

<sup>9</sup>Note that the accuracy of the model is not that critical, as long as the same mapping is used by both users. It is clear that the success of a scheme that utilizes RSSI's is dependent on channel reciprocity, but our algorithm does not rule out the use of other means of measuring the distances.

measurements  $\hat{\mathbf{d}}_1, \hat{\mathbf{d}}_2$  at the legitimate nodes and  $\hat{\mathbf{d}}_{2e}$  at node  $e$ , each of size  $n$ -samples, are provided in Figure 11. Recall that  $\mathbf{d}_{1e}$  is known perfectly at the eavesdropper.

Recall from Section III-B that in case of the lack of mobility statistics and GLI at the legitimate nodes, we generate keys based on 1-D relative distance information, instead of 2-D relative location information. Therefore, we skip Viterbi algorithm, and consider 2-bit uniform quantization function

$$\psi(d, \Delta) = \arg \min_k |k - d|, k \in \{3u\}, u \in \mathbb{Z}$$

and use a  $m = 2$ -bit Gray coder<sup>10</sup> to obtain initial binary sequences  $\mathbf{v}_1, \mathbf{v}_2$  and  $\mathbf{v}_e$ , each of size  $nm = 2000$  bits. In Figure 13, we provide  $\mathbf{v}_1$ , along with the bit mismatches in node 2, i.e.,  $(\mathbf{v}_1 \oplus \mathbf{v}_2)$ , and the bit mismatches in node  $e$ , i.e.,  $(\mathbf{v}_1 \oplus \mathbf{v}_e)$  before information reconciliation. The bit mismatch rates are  $(BMR(\mathbf{v}_1, \mathbf{v}_2)) = 0.1210$  and  $(BMR(\mathbf{v}_1, \mathbf{v}_e)) = 0.3740$ . Then, we use Cascade reconciliation protocol to correct bit mismatches at node 2. The legitimate nodes obtain  $\mathbf{u}_1$  and  $\mathbf{u}_2$ , where bit mismatches  $(\mathbf{u}_1 \oplus \mathbf{u}_2)$  at the legitimate node 2 are shown in Figure 13, The bit mismatches at legitimate nodes are almost completely corrected during reconciliation, as  $(BMR(\mathbf{w}_1, \mathbf{w}_2)) = 0.001$ . However,  $T = 1504$  message bits are exchanged each way on the public channel, and revealed to node  $e$ . Finally, the legitimate nodes compress their bit sequences  $\mathbf{u}_1$  and  $\mathbf{u}_2$  using universal compression to obtain compressed sequences  $\mathbf{q}_1$  and  $\mathbf{q}_2$ , each of size 1448 bits, hence compression ratio is  $\alpha = 0.724$ . Finally, the legitimate nodes obtain apply privacy amplification to the compressed sequences to obtain shorter messages  $\mathbf{k}_1$  and  $\mathbf{k}_2$ , of size  $nR$ . Choosing  $R = 0.30$  bits /slot is sufficient for perfect secrecy, according to (15), which corresponds to 0.15 bits /second. Note that, in these experiments we take one observation per 2 seconds. This rate can be increased by taking observations more frequently. In Table III we provide the results of the NIST randomness tests applied to key sequence  $\mathbf{k}_1$ . Here, a value greater than 0.01 is considered as a pass [27]. It can be observed that  $\mathbf{k}_1$  passes all the randomness tests.

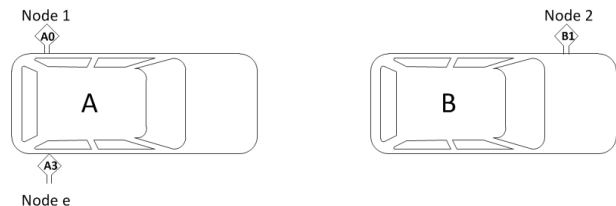


Fig. 12: Antenna placement on vehicles

## VII. CONCLUSION

In this paper, we developed an algorithm that generates keys based on the relative localization information between legitimate nodes in mobile wireless networks. In the first

<sup>10</sup>Recall from Section III-C that  $m$  is chosen largest possible such that (11) is satisfied.

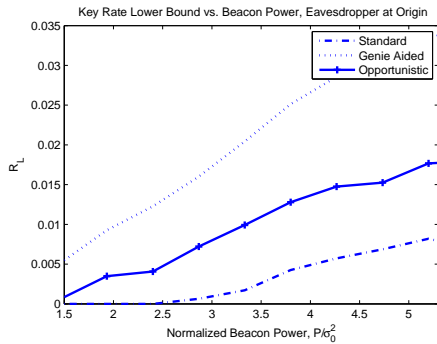


Fig. 9: Opportunistic beacon exchange, no GLI

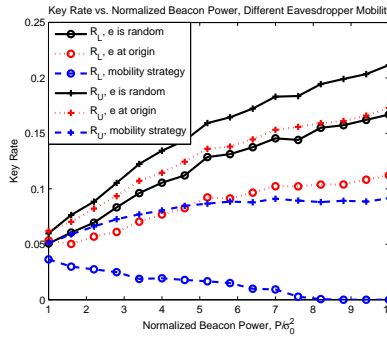


Fig. 10: Effect of eavesdropper mobility on the key rate

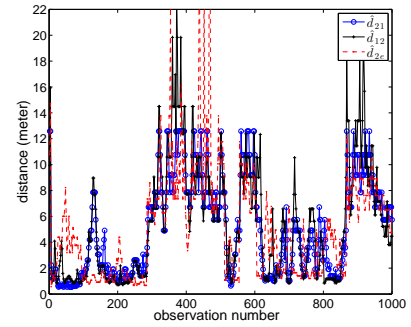


Fig. 11: Distance observations for free-way data

Test type	result
Frequency	0.534146
BlockFrequency	0.911413
CumulativeSums	0.534146
Rank	0.066882
FFT	0.350485
LinearComplexity	0.122325

TABLE III: Randomness test results for the key generation algorithm

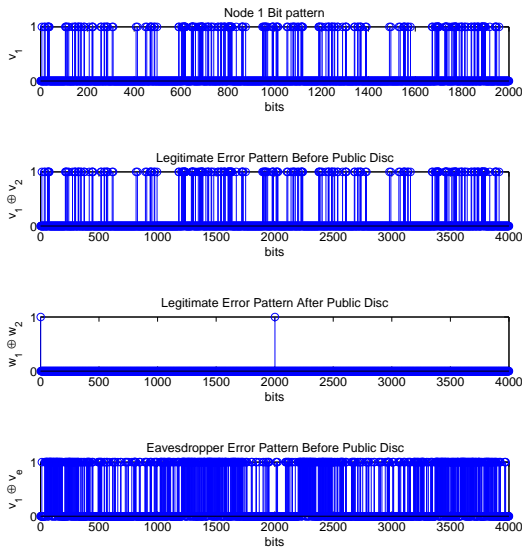


Fig. 13: Bit error patterns of nodes before and after public discussion

stage, legitimate nodes perform localization. Then, the nodes' relative distance estimates are converted to a binary sequence, out of which the nodes agree on some initial key bits with high probability by public discussion. Finally, universal data compression and privacy amplification are performed on the key bits to obtain the secret key with a low bit mismatch rate at the legitimate nodes as well as a low information leakage rate to the eavesdropper. We studied the information theoretic limits of secret key generation, and characterized lower and upper bounds of key rates utilizing results from the source

model of secrecy, for the cases in which the nodes are/are not capable of observing their global locations. Focusing on the special case where the observation noise is i.i.d. Gaussian, we studied the beacon power asymptotics, and showed that when the eavesdropper cannot observe the angle information, the secret key rate grows unboundedly, whereas with an angle observation at eavesdropper, key rate remains bounded. We developed an opportunistic beacon exchange component, integrated it to our algorithm, and showed that non-zero secret key rates are achievable even when the eavesdropper is more capable on average. We also tested our algorithm on a vehicular setting, and showed that non-zero key rates are achievable in practice, even under extremely pessimistic settings, and without any a-priori statistical assumptions on the mobility model. Our current investigations are mainly focused on 1) common secret key generation among multiple nodes in a wireless network, and 2) application to an unauthenticated network, where the eavesdropper interferes with the localization process.

## APPENDIX A ON KEY GENERATION ALGORITHM

### A. Viterbi Algorithm

The terms  $\tilde{s}_j^\Delta$  are obtained iteratively using Viterbi algorithm as follows. Let

$$\chi_j(s^\Delta[i]) \triangleq \arg \max_{s^\Delta[1], \dots, s^\Delta[i]} \mathbb{P}(s^\Delta[1], \dots, s^\Delta[i] | o_j[1], \dots, o_j[i])$$

denote the most likely sequence of node  $j$  based on its observations up to slot  $i$ . Then, Viterbi algorithm follows from the following relation for any  $i$ ,

$$f(\chi_j(s^\Delta[i]), o_j[1], \dots, o_j[i]) = f(\chi_j(s^\Delta[i-1]), o_j[1], \dots, o_j[i-1]) \times \mathbb{P}(s^\Delta[i] | s^\Delta[i-1]) f(o_j[i] | s^\Delta[i]). \quad (32)$$

Iterating over  $n$  slots, the nodes  $j \in \{1, 2\}$  find

$$\tilde{s}_j^\Delta = \arg \max_{\chi_j(s^\Delta[n])} \mathbb{P}(\chi_j(s^\Delta[n]) | o_j) \quad (33)$$



## B. Cascade Algorithm

We provide a brief sketch of the cascade reconciliation protocol. The protocol operates over  $P$  passes. Prior to first pass, we initialize  $m_0 = m$ ,

$$u_{j,0}[i] = v_j[i], \quad \forall i, j$$

and  $\mathbf{u}_{j,0} = \{u_{j,0}[i]\}_{i=1}^n$ . In the first pass, binary sequences  $\mathbf{u}_{j,0}$  are re-divided into  $n_1$  blocks  $\mathbf{u}_{j,1}[1] \dots, \mathbf{u}_{j,1}[n_1]$  of  $m_1$  bits such that  $n_1 m_1 = n m_0$ , and

$$u_{j,1}[i] \triangleq [v_j[(i-1)m_1] \dots v_j[im_1 - 1]]$$

and

$$\mathbf{u}_{j,1} \triangleq [u_{j,1}[1] \dots u_{j,1}[n_1]].$$

Node 1, the master node, calculates parity bits  $C_1[i]$  from each  $m_1$  bit block  $u_{1,1}[i]$  as

$$C_1[i] = \text{parity}(u_{1,1}[i])$$

and communicates  $[C_1[1] \dots C_1[n_1]]$  to node 2 over the public channel. Node 2 similarly calculates the parity bits  $C_2[i]$  from  $\mathbf{u}_{2,1}[i]$ . If the parity in block  $i$  does not match, i.e.,  $C_1[i] \neq C_2[i]$ , then it indicates that there are odd number of errors in block  $i$ . In that case, a recursive protocol referred to in [28] as BINARY is executed, which is essentially recursively dividing block  $i$  to sub-blocks and comparing the parities of the sub-blocks until a bit in error is found. When all the blocks  $1 \dots n_1$  are compared, they all contain even number of errors, and the first pass is over. In the subsequent passes  $p > 1$ , the bit sequences  $\mathbf{u}_{j,p-1}$  are shuffled such that

$$\mathbf{u}_{j,p} \triangleq g_p(\mathbf{u}_{j,p-1}),$$

Here,  $g_p$  is randomly and uniformly chosen from set of permutation functions by the master node, and broadcast on the public channel. The parity exchange process on each block  $u_{j,p}[i], i \in \{1 \dots n_p\}$  is similarly repeated. Note that, when an error is found and corrected in  $p$ 'th pass, the blocks containing that corrected bit in the  $p-1$  passes contain odd number of errors. Therefore, the parity exchange process is repeated on the smallest sub-block of the among those blocks.

This process is repeated for  $P$  passes, and,  $T$  bits ( $C_j[1] \dots C_j[T]$ ) are exchanged each way between the legitimate nodes by the end of the Cascade protocol. Due to the interactive nature of the protocol, the number  $T$  depends on the initial bit mismatch rate between the sequences  $\mathbf{v}_1$  and  $\mathbf{v}_2$ , and the number of passes  $P$ . We choose Cascade algorithm parameters as suggested in [28]:

- $m_1$  is chosen such that  $\frac{1}{n_1} \sum_{i=1}^{n_1} \mathbf{1}(u_{1,0}[i] \neq u_{2,0}[i]) = 0.7$ , i.e., 70% of the divided chunks  $u_{j,0}[i]$  are not identical. Recall that the choice of  $m_1$  determines  $n_1$  since  $m_1 n_1 = m_0 n$
- $m_p = 2m_{p-1}$  for  $p > 1$
- $P = 4$

For simplicity, we drop the number of iterations for the key sequences generated at the end of Cascade reconciliation protocol and denote the resulting key sequences with:  $\mathbf{u}_j \triangleq \mathbf{u}_{j,P}$ .

## C. Choice of Rate $R$

In three steps, we approximate  $R^*$  in (14).

1) Consider the case  $\alpha = 1$ , i.e., the sequences  $\mathbf{u}_j$  are perfectly compressed. We assume that the eavesdropper follows a strategy that is better than the optimal strategy it can perform, as follows. In localization phase, we assume that the eavesdropper also uses the Viterbi Algorithm to obtain  $\hat{\mathbf{s}}_e^\Delta$ , and converts it to a bit sequence  $\mathbf{v}_e$  of size  $nm$ . Recall that in the public discussion phase, node  $j \in \{1, 2\}$  obtains  $\hat{\mathbf{s}}_j^\Delta$  based on the observations  $\mathbf{o}_j$  and obtains the bit sequence  $\mathbf{v}_j$ . Then, cascade reconciliation protocol is initiated, where node 1 and 2 sends each other binary messages  $[C_1[1], \dots, C_1[T]]$  and  $[C_2[1], \dots, C_2[T]]$  over the public channel, to agree on initial keys  $\mathbf{u}_1$  and  $\mathbf{u}_2$ , each of size  $nm$  such that (10) holds. This approach is suboptimal compared to the soft decoding scheme in which the bit sequence  $\mathbf{u}_2$  is decoded directly based on the observations  $\mathbf{o}_2$  and the the binary messages. Therefore, we assume that the eavesdropper does not follow the sub-optimal approach. Instead, we make the highly optimistic assumption for the eavesdropper that it corrects  $T$  bits that was in error; equal to the number of parity bits exchanged each way during cascade protocol. Based on these assumptions,  $R^*$  is approximated as

$$\begin{aligned} R_1^* &= \frac{1}{n} H(\mathbf{q}_1 | \hat{\mathbf{s}}_e^\Delta, \{C_1[t], C_2[t]\}_{t=1}^T) \\ &\geq \frac{1}{n} (H(\mathbf{v}_1 | \mathbf{v}_e) - T), \end{aligned} \quad (34)$$

which follows from the fact that public broadcast of the messages  $\{C_1[t], C_2[t]\}_{t=1}^T$  can at most reveal  $T$  bits from  $\mathbf{u}_1$ .

2) To approximately evaluate  $H(\mathbf{v}_1 | \mathbf{v}_e)$ , we treat  $\mathbf{v}_e$  as if it is formed by passing  $\mathbf{v}_1$  through a binary symmetric channel, with crossover probability  $\text{BMR}_e$ . Then,  $H(\mathbf{v}_1 | \mathbf{v}_e) \approx nm(1 - \text{BSC}(\text{BMR}_e))$ , where

$$\begin{aligned} \text{BSC}(\text{BMR}_e) &= 1 + \text{BMR}_e \log(\text{BMR}_e) \\ &\quad + (1 - \text{BMR}_e) \log(1 - \text{BMR}_e) \end{aligned}$$

is the capacity of a binary symmetric channel with crossover probability of  $\text{BMR}_e$ . Hence, (34) becomes

$$\begin{aligned} R_2^* &= -\text{BMR}_e \log(\text{BMR}_e) \\ &\quad - (1 - \text{BMR}_e) \log(1 - \text{BMR}_e) - \frac{T}{n} \end{aligned} \quad (35)$$

when  $\alpha = 1$ .

3) When  $\alpha < 1$ , we scale  $R_2^*$  with the compression ratio to obtain (15).

## APPENDIX B

### ON OPPORTUNISTIC BEACON EXCHANGE

We do not directly use (28) for beacon transmission decisions due to certain challenges. Here, we address them, and justify why we use (31) instead. The first issue is that it is difficult to verify Condition (28). To see whether there exists a valid probability density function  $\hat{f}$  that satisfies (28), we can pose the problem as that of calculus of variations:

$$\mu = \min_{\hat{f}} \left| f(\hat{d}_1[i] | d_{12}[i]) - \right.$$

$$\int_{x=(\hat{d}_{1e}[i], \hat{d}_{2e}[i], \hat{\phi}_e[i])} f(x|d_{12}[i])\tilde{f}(\hat{d}_1[i]|x)dx \Big|$$

subject to :  $\int \tilde{f}(u)du = 1.$

If  $\mu = 0$ , then the legitimate nodes' observations are stochastically degraded version of the eavesdropper's observations. However, due to the fact that there may exist no closed form expression for  $f(\hat{d}_{1e}[i], \hat{d}_{2e}[i], \hat{\phi}_e[i]|d_{12}[i])$ , this problem can be highly complex. Instead, in our algorithm, the legitimate nodes make their decisions based on an approximate version of (28) at the expense of some loss in the key rate. Define  $\hat{d}_e[i]$  as

$$\hat{d}_e[i] = \sqrt{[\hat{d}_{1e}[i]^2 + \hat{d}_{2e}[i]^2 - 2\hat{d}_{1e}[i]\hat{d}_{2e}[i]\cos\hat{\phi}_e[i]]^+} \quad (36)$$

which corresponds to the cosine law estimate of  $d_{12}[i]$  of the eavesdropper. Through a sequence of approximations on  $\hat{d}_e[i]$  as described in Appendix B-A, we end up with

$$\hat{d}_e^*[i] = d_{12}[i] + w_e[i], \quad (37)$$

where  $w_e[i] \sim \mathcal{N}\left(0, \frac{\rho_e(A[i]+B[i])}{P}\right)$ , such that  $A[i]$ , given in (29) is the uncertainty that comes from the distance observation errors, and  $B[i]$ , given in (30) is the uncertainty that comes from the angle estimate error.

Note that the idea behind the described approximation is linearization of  $\hat{d}_e[i]$  and hence the approximation becomes more and more accurate as the beacon power increases (i.e., in the high signal to noise ratio regime).

In our algorithm, the legitimate nodes use the term  $\hat{d}_e^*[i]$  for beacon transmission decisions. Clearly,  $d_{12}[i] \rightarrow (\hat{d}_{1e}[i], \hat{d}_{2e}[i], \hat{\phi}_e[i]) \rightarrow \hat{d}_e^*[i]$  forms a Markov chain. Consequently, when  $\hat{d}_{1e}[i]$  and  $\hat{d}_{2e}[i]$  are stochastically degraded versions of  $\hat{d}_e^*[i]$ , they are also stochastically degraded versions of the eavesdropper observations  $(\hat{d}_{1e}[i], \hat{d}_{2e}[i], \hat{\phi}_e[i])$ , hence the condition (28) is satisfied. Since the legitimate nodes' observations follow the distributions

$$\hat{d}_j[i] \sim \mathcal{N}\left(d_{12}[i], \frac{\gamma(d_{12}[i])\rho_j}{P}\right)$$

for  $j \in \{1, 2\}$ , the condition

$$\rho_{\max}\gamma(d_{12}[i]) > \rho_e(A[i] + B[i]) \quad (38)$$

would be sufficient to verify that the actual node measurement is more degraded than the eavesdropper measurement<sup>11</sup>. Note that the legitimate nodes cannot make use of (38) for beacon transmission decisions directly, since they only have the statistics of the eavesdropper location, and they do not know the parameters  $A[i]$ ,  $B[i]$  and  $d_{12}[i]$  exactly. However, using the statistical knowledge, they can calculate the probability of event (38), conditioned on their observations, which is (31). Therefore, (31) is used as a basis for beacon transmission decisions.

<sup>11</sup>Note however that converse is not true since  $\hat{d}_e^*[i]$  is not a sufficient statistic of  $(\hat{d}_{1e}[i], \hat{d}_{2e}[i], \hat{\phi}_e[i])$ .

### A. Linear Approximation for $\hat{d}_e$

In this part, we explain how we obtain  $\hat{d}_e^*[i]$  from  $\hat{d}_e[i]$  via a sequence of linear approximations. In what follows, we drop the time index  $[i]$  for simplicity.

$$\begin{aligned} \hat{d}_e &= \left( \left[ (d_{1e} + w_{1e})^2 + (d_{2e} + w_{2e})^2 - \right. \right. \\ &\quad \left. \left. 2(d_{1e} + w_{1e})(d_{2e} + w_{2e})\cos(\phi_e + w_{\phi_e}) \right]^+ \right)^{0.5} \\ &\approx \left( \left[ d_{1e}^2 + d_{2e}^2 + 2d_{1e}w_{1e} + 2d_{2e}w_{2e} \right. \right. \\ &\quad \left. \left. - 2d_{1e}d_{2e}\cos(\phi_e + w_{\phi_e}) - 2d_{1e}w_{2e}\cos(\phi_e + w_{\phi_e}) \right. \right. \\ &\quad \left. \left. - 2d_{2e}w_{1e}\cos(\phi_e + w_{\phi_e}) \right]^+ \right)^{0.5} \end{aligned} \quad (39)$$

$$\begin{aligned} &\approx \left( \left[ d_{12}^2 + 2d_{1e}d_{2e}\sin(\phi_e)w_{\phi_e} + 2w_{1e}(d_{1e} - d_{2e}\cos\phi_e) \right. \right. \\ &\quad \left. \left. + 2w_{2e}(d_{2e} - d_{1e}\cos\phi_e) \right]^+ \right)^{0.5} \end{aligned} \quad (40)$$

$$\begin{aligned} &\approx d_{12} + \frac{1}{d_{12}^2} \left( d_{1e}d_{2e}\sin(\phi_e)w_{\phi_e} + \right. \\ &\quad \left. w_{1e}(d_{1e} - d_{2e}\cos\phi_e) + w_{2e}(d_{2e} - d_{1e}\cos\phi_e) \right) \end{aligned} \quad (41)$$

$$= d_{12} + w_x, \quad (42)$$

where (39) follows from omitting the higher order terms  $(w_{1e}^2 + w_{2e}^2 + 2w_{1e}w_{2e}\cos(\phi_e + w_{\phi_e}))$ , since their variances scale with  $O(\frac{1}{P^2})$ ; (40) follows from the approximation

$$\begin{aligned} \cos(\phi_e + w_{\phi_e}) &= \cos(\phi_e)\cos(w_{\phi_e}) - \sin(\phi_e)\sin(w_{\phi_e}) \\ &\approx \cos(\phi_e) - w_{\phi_e}\sin(\phi_e), \end{aligned}$$

which becomes accurate as  $w_{\phi_e} \searrow 0$ ; and (41) follows from the linear approximation  $\sqrt{1+x} \approx 1 + \frac{x}{2}$  for  $x \ll 1$ , which is accurate for high signal to noise ratio, i.e.,  $w_{\phi_e}, w_{1e}$ , and  $w_{2e}$  are all small (close to 0) with high probability. Note that, the overall noise term follows the distribution  $w_x \sim \mathcal{N}\left(0, \frac{\rho_e(A+B)}{P}\right)$ .

### B. Forward Algorithm

Due to the Markov assumption on the mobility model, the states  $s^\Delta[i-1] \rightarrow s^\Delta[i] \rightarrow s^\Delta[i+1]$  form a Markov chain. Also, since the observations  $o_j[i]$  are Gaussian, with a variance depending solely on the current state  $s^\Delta[i]$ ,  $o_j[i]$  is independent of  $\{s^\Delta[k]\}_{k \neq i}$  given  $s[i]$ . Therefore,  $s^\Delta[i]$ 's and  $o_j[i]$ 's form a hidden Markov chain as depicted in Figure 14. Forward Algorithm follows from the simple observation that for any slot  $i$ ,

$$\begin{aligned} f(o_j[1], \dots, o_j[i], s^\Delta[i]) &= \int f(o_j[1], \dots, o_j[i-1], \\ &\quad s^\Delta[i-1])\mathbb{P}(s^\Delta[i]|s^\Delta[i-1])f(o_j[i]|s^\Delta[i])ds^\Delta[i-1]. \end{aligned} \quad (43)$$

The term  $\mathbb{P}(s^\Delta[i]|s^\Delta[i-1])$  is called state transition probability, and is independent on current time slot  $i$ , since the mobility model is stationary. The term  $f(o_j[i]|s^\Delta[i])$  is called emission density, which is Gaussian, as described by (20)-(22). Thus (43) gives us an iterative relationship to calculate

$f(o_j[1], \dots, o_j[i], s^\Delta[i])$  using  $f(o_j[1], \dots, o_j[i-1], s^\Delta[i-1])$ . Iterating over (43) for  $n$  slots, we obtain  $f(\mathbf{o}_j, \mathbf{s}^\Delta)$ . Recall that  $\mathbf{s}^\Delta = [\mathbf{1}_1^\Delta, \mathbf{1}_2^\Delta, \mathbf{1}_e^\Delta]$ , the quantized states, contains quantized version of all the distance and angle information in (31), e.g.,  $(\hat{\mathbf{d}}_{12}^\Delta, \hat{\mathbf{d}}_{je}^\Delta, \hat{\phi}_e^\Delta)$ . Hence, the probability in (31) can be efficiently calculated.

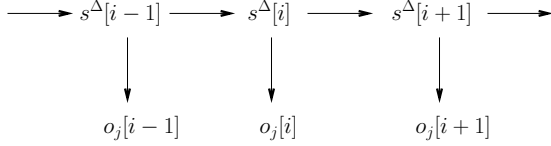


Fig. 14: The hidden Markov structure

### APPENDIX C

#### PROOFS OF THEOREMS IN SECTION V-A

##### A. Proof of Theorem 2

We first provide several lemmas that will be useful when proving the theorem.

*Lemma 1:* Let  $x$  and  $y$  be random variables. Then,

$$\text{Var}(x+y) \leq 2\text{Var}(x) + 2\text{Var}(y). \quad (44)$$

If  $x$  and  $y$  are independent, then

$$\text{Var}(x+y) = \text{Var}(x) + \text{Var}(y). \quad (45)$$

*Proof:* When  $x$  and  $y$  are not independent,

$$\begin{aligned} \text{Var}(x+y) &= \text{Var}(x) + \text{Var}(y) + 2\text{Cov}(x,y) \\ &\leq \text{Var}(x) + \text{Var}(y) + 2\sqrt{\text{Var}(x)\text{Var}(y)} \\ &\leq 2\text{Var}(x) + 2\text{Var}(y). \end{aligned} \quad (46)$$

where (46) follows from the fact that  $\text{Var}(x) + \text{Var}(y) \geq 2\sqrt{\text{Var}(x)\text{Var}(y)}$ . When  $x$  and  $y$  are independent,  $\text{Cov}(x,y) = 0$ , implying the result. ■

*Lemma 2:* Let  $x$  be a random variable such that  $\mathbb{E}[x] \geq \mu$ , where  $\mu > -1$ . Let  $\alpha = \frac{\sqrt{1+\mu}}{1+\mu}$ . Then,  $\text{Var}(\sqrt{1+x}^+) \leq \text{Var}(\alpha x)$ .

*Proof:* Assume  $\mathbb{E}[x] = \mu'$ , where  $\mu' \geq \mu$ . Let  $\alpha' = \frac{\sqrt{1+\mu'}}{1+\mu'}$ . Let us define  $f_1(x) \triangleq \sqrt{1+x}^+$ , and  $f_2(x) \triangleq \alpha'(1+x)$ . Note that,

$$\text{Var}(\sqrt{1+x}^+) = \text{Var}(f_1(x)) \leq \mathbb{E}[(f_1(x) - \mathbb{E}[f_2(x)])^2]$$

since the centralized second moment is minimized around the mean. Also,

$$\text{Var}(\alpha x) \geq \text{Var}(\alpha' x) = \text{Var}(f_2(x))$$

since  $\mu' \geq \mu$ , and  $\alpha' \leq \alpha$ . Therefore, it suffices to show that  $\forall x$ ,

$$|f_1(x) - \mathbb{E}[f_2(x)]| \leq |f_2(x) - \mathbb{E}[f_2(x)]| \quad (47)$$

$$= |f_2(x) - \sqrt{1+\mu'}|. \quad (48)$$

holds.

i) First note that  $f_1(\mu') = f_2(\mu') = \sqrt{1+\mu'}$ . Therefore, the condition (48) is satisfied for  $x = \mu'$ .

ii) For  $x > \mu'$ ,

$$f_1(x) \leq f_1(\mu') + f_1'(\mu')(x - \mu') \quad (49)$$

$$\leq \sqrt{1+\mu'} + \alpha(x - \mu') = f_2(x)$$

where  $f_1'(\mu')$  is the first derivative of  $f_1(x)$  at point  $x = \mu'$ . (49) follows from the fact that  $f_1(x)$  is a strictly concave function in the interval  $[-1, \infty)$ . Therefore, condition (48) is satisfied for  $x > \mu'$ .

iii) Combining the facts that  $f_1(x)$  is a strictly concave function of  $x$  in the interval  $[-1, \infty)$ ;  $f_2(x)$  is linear;  $f_1(-1) = f_2(-1)$ ; and  $f_1(\mu') = f_2(\mu')$ , we can see that  $\sqrt{1+\mu'} > f_1(x) \geq f_2(x)$  when  $-1 < x < \mu'$ . Therefore, condition (48) is satisfied for  $-1 < x < \mu'$ . iv) When  $x < -1$ ,  $f_1(x) = 0$  and  $f_2(x) < 0$ , therefore, condition (48) is satisfied. This concludes the proof. ■

*Lemma 3:* Let  $x, y$  be random variables. Then,

$$\text{Var}\left(\mathbb{E}\left[1 - \sqrt{(1+x)^+} \mid y\right]\right) \leq \mathbb{E}\left[\left(\mathbb{E}[|x| \mid y]\right)^2\right].$$

*Proof:* Note that

$$\begin{aligned} \text{Var}\left(\mathbb{E}\left[1 - \sqrt{(1+x)^+} \mid y\right]\right) \\ \leq \mathbb{E}\left[\mathbb{E}\left[1 - \sqrt{(1+x)^+} \mid y\right]^2\right]. \end{aligned}$$

Since for any  $x$ ,  $|1 - \sqrt{(1+x)^+}| \leq |x|$ ,

$$\left|\mathbb{E}\left[1 - \sqrt{(1+x)^+} \mid y\right]\right| \leq \mathbb{E}[|x| \mid y]$$

is satisfied for any  $y$ , which completes the proof. ■

Now, we can proceed with the proof of the theorem. Assume without loss of generality that  $\rho_{\min} = \min(\rho_1, \rho_2) = \rho_1$ . When  $\hat{\phi}_e \neq \emptyset$ , we can obtain an upper bound on the secret key rate as follows.

$$\begin{aligned} R_U &= \lim_{n \rightarrow \infty} \frac{1}{n} I(\hat{\mathbf{d}}_1; \hat{\mathbf{d}}_2 | \hat{\mathbf{d}}_{1e}, \hat{\mathbf{d}}_{2e}, \hat{\phi}_e) \\ &\leq \lim_{n \rightarrow \infty} \frac{1}{n} (h(\hat{\mathbf{d}}_1 | \hat{\mathbf{d}}_{1e}, \hat{\mathbf{d}}_{2e}, \hat{\phi}_e) - h(\hat{\mathbf{d}}_1 | \mathbf{d}_{12})) \quad (50) \\ &\leq \lim_{n \rightarrow \infty} \frac{1}{n} \sum_{i=1}^n \left( h(\hat{d}_1[i] | \hat{d}_{1e}[i], \hat{d}_{2e}[i], \hat{\phi}_e[i]) - \right. \\ &\quad \left. h(\hat{d}_1[i] - d_{12}[i] | d_{12}[i]) \right) \\ &= h(\hat{d}_1 | \hat{d}_{1e}, \hat{d}_{1e}, \hat{\phi}_e) - h(\hat{d}_1 - d_{12} | d_{12}) \quad (51) \end{aligned}$$

where (50) follows from the fact that  $\hat{\mathbf{d}}_1 \rightarrow \mathbf{d}_{12} \rightarrow (\hat{\mathbf{d}}_2, \hat{\mathbf{d}}_{1e}, \hat{\mathbf{d}}_{2e}, \hat{\phi}_e)$  forms a Markov chain, and (51) follows from the fact that all of the random variables  $\hat{d}_1[i], \hat{d}_{1e}[i], \hat{d}_{2e}[i], \hat{\phi}_e[i]$  have a stationary distribution, denoted as  $\hat{d}_1, \hat{d}_{1e}, \hat{d}_{2e}$  and  $\hat{\phi}_e$ , respectively. The second term in (51) can be directly found as

$$h(\hat{d}_1 - d_{12} | d_{12}) = \frac{1}{2} \mathbb{E} \left[ \log \left( \frac{\gamma(d_{12}) \rho_1}{P} \right) \right] \quad (52)$$

from the definition of  $\hat{d}_1[i]$ . Now, we bound the first term in (51). Let us define

$$\hat{d}_e \triangleq \sqrt{[\hat{d}_{1e}^2 + \hat{d}_{2e}^2 - 2\hat{d}_{1e}\hat{d}_{2e} \cos(\hat{\phi}_e)]^+}.$$

Then,

$$h(\hat{d}_1 | \hat{d}_{1e}, \hat{d}_{2e}, \hat{\phi}_e) \leq h(\hat{d}_1 | \hat{d}_e) \leq h(\hat{d}_1 - \hat{d}_e). \quad (53)$$

Note that for a given variance, Gaussian distribution maximizes the entropy. Therefore, the entropy of a Gaussian random variable that has a variance identical to that of  $\hat{d}_1 - \hat{d}_e$  will be an upper bound for (53). We proceed as follows.

$$\begin{aligned} \text{Var}(\hat{d}_1 - \hat{d}_e) &= \mathbb{E}[\text{Var}(\hat{d}_1 - \hat{d}_e | d_{12}, d_{1e}, d_{2e})] \\ &\quad + \text{Var}(\mathbb{E}[\hat{d}_1 - \hat{d}_e | d_{12}, d_{1e}, d_{2e}]), \end{aligned} \quad (54)$$

where (54) follows from the fact that for any dependent random variables  $x$  and  $y$ ,  $\text{Var}(x) = \mathbb{E}[\text{Var}(x|y)] + \text{Var}(\mathbb{E}[x|y])$ . We now find an upper bound on the first term of (54). Note that,

$$\begin{aligned} \text{Var}(\hat{d}_1 - \hat{d}_e | d_{12}, d_{1e}, d_{2e}) &= \text{Var}(\hat{d}_1 | d_{12}) \\ &\quad + \text{Var}(\hat{d}_e | d_{12}, d_{1e}, d_{2e}) \end{aligned} \quad (55)$$

due to Lemma 1, since  $\hat{d}_1 \rightarrow (d_{12}, d_{1e}, d_{2e}) \rightarrow (\hat{d}_{1e}, \hat{d}_{2e}, \hat{\phi}_e) \rightarrow \hat{d}_e$  forms a Markov chain, and the fact that  $\hat{d}_1$  is independent of  $d_{1e}, d_{2e}$  given  $d_{12}$ . The first term in (55) is equal to

$$\text{Var}(\hat{d}_1 | d_{12}) = \text{Var}(w_1 | d_{12}) = \frac{\gamma(d_{12})\rho_1}{P}. \quad (56)$$

We bound the second term in (55) as follows. Let us define  $\kappa$  as

$$\begin{aligned} \kappa &\triangleq \frac{1}{d_{12}^2} \left( 2(d_{1e} - d_{2e} \cos(\hat{\phi}_e))w_{1e} + w_{1e}^2 \right. \\ &\quad \left. + w_{2e}^2 + 2(d_{2e} - d_{1e} \cos(\hat{\phi}_e))w_{2e} \right. \\ &\quad \left. + 2d_{1e}d_{2e}(\cos(\phi_e) - \cos(\hat{\phi}_e)) - 2w_{1e}w_{2e} \cos(\hat{\phi}_e) \right). \end{aligned}$$

Then,

$$\begin{aligned} &\text{Var}(\hat{d}_e | d_{12}, d_{1e}, d_{2e}) \\ &= \text{Var} \left\{ \left( \left[ d_{1e}^2 + d_{2e}^2 + 2(d_{1e} - d_{2e} \cos \hat{\phi}_e)w_{1e} + \right. \right. \right. \\ &\quad \left. \left. \left. 2(d_{2e} - d_{1e} \cos \hat{\phi}_e)w_{2e} - 2d_{1e}d_{2e} \cos \hat{\phi}_e + w_{1e}^2 \right. \right. \right. \\ &\quad \left. \left. \left. + w_{2e}^2 - 2w_{1e}w_{2e} \cos \hat{\phi}_e \right]^+ \right)^{0.5} | d_{12}, d_{1e}, d_{2e} \right\} \quad (57) \\ &\leq d_{12}^2 \text{Var}(\sqrt{[1 + \kappa]^+}), \quad (58) \end{aligned}$$

where (57) follows due to the definitions of  $\hat{d}_{1e}$ ,  $\hat{d}_{2e}$  and  $\hat{\phi}_e$ . (58) follows due to definition of  $\kappa$ , and the cosine law  $d_{12}^2 = d_{1e}^2 + d_{2e}^2 - 2d_{1e}d_{2e} \cos(\phi_e)$ . Now we will apply Lemma 2 to bound (58). First, note that

$$\begin{aligned} \mathbb{E}[\kappa] &= \frac{1}{d_{12}^2} \mathbb{E} \left[ w_{1e}^2 + w_{2e}^2 - 2d_{1e}d_{2e}(\cos \phi_e - \cos \hat{\phi}_e) \right] \\ &\geq \frac{1}{Pd_{12}^2} \mathbb{E} \left[ w_{1e}^2 + w_{2e}^2 - 2d_{1e}d_{2e}|w_{\phi_e}| \right] \\ &\geq \frac{\rho_e}{Pd_{12}^2} \mathbb{E} \left[ \gamma(d_{1e}) + \gamma(d_{2e}) - 2d_{1e}d_{2e} \sqrt{\frac{2P\gamma_{\phi}(d_{1e}, d_{2e})}{\pi\rho_e}} \right], \end{aligned} \quad (59)$$

where (59) follows from the fact that since  $w_{\phi_e}$  is zero mean Gaussian,  $|w_{\phi_e}|$  follows a Half-normal distribution with  $\mathbb{E}(|w_{\phi_e}|) = \sqrt{\frac{2\gamma_{\phi}(d_{1e}, d_{2e})\rho_e}{P\pi}}$ . We can choose  $P_1$  such that for

any beacon power  $P > P_1$ ,  $\mathbb{E}[x] > -\frac{3}{4}$ . Let  $\mu = -\frac{3}{4}$ , and  $\alpha = \frac{\sqrt{1+\mu}}{1+\mu} = 2$ . Due to Lemma 2, we obtain

$$\begin{aligned} d_{12}^2 \text{Var}(\sqrt{[1 + \kappa]^+}) &\leq d_{12}^2 \text{Var}(\alpha\kappa) \\ &\leq \frac{4\alpha^2}{d_{12}^2} \left( \text{Var}(2(d_{1e} - d_{2e} \cos(\hat{\phi}_e))w_{1e}) \right. \end{aligned} \quad (60)$$

$$\begin{aligned} &\quad \left. + \text{Var}(2(d_{2e} - d_{1e} \cos(\hat{\phi}_e))w_{2e}) \right. \\ &\quad \left. + \text{Var}(2d_{1e}d_{2e}(\cos(\phi_e) - \cos(\hat{\phi}_e))) \right. \\ &\quad \left. + \text{Var}(2w_{1e}w_{2e} \cos(\hat{\phi}_e)) + \text{Var}(w_{1e}^2) + \text{Var}(w_{2e}^2) \right) \end{aligned}$$

$$\leq \mathbb{E} \left[ \frac{16\rho_e}{Pd_{12}^2} \left( 4(d_{1e} + d_{2e})^2(\gamma(d_{1e}) + \gamma(d_{2e})) \right. \right. \quad (61)$$

$$\left. \left. + 4(d_{1e}d_{2e})^2\gamma_{\phi}(d_{1e}, d_{2e}) + o\left(\frac{1}{P}\right) \right) \right], \quad (62)$$

where (60) follows from applying Lemma 1 to  $\text{Var}(\kappa)$  twice, and (62) follows from the fact that

$$\text{Var}(2(d_{ie} - d_{je} \cos(\hat{\phi}_e))w_{ie}) \leq \text{Var}(2(d_{ie} + d_{je})w_{ie})$$

for  $i, j \in \{1, 2\}$ , and

$$\begin{aligned} &\text{Var}(2d_{1e}d_{2e}(\cos(\phi_e) - \cos(\hat{\phi}_e))) \\ &= \text{Var}(2d_{1e}d_{2e}(\cos(\phi_e) - \cos(\phi_e + w_{\phi}))) \\ &\leq \text{Var}(2d_{1e}d_{2e}w_{\phi}). \end{aligned}$$

Now, we find an upper bound for the second term of (54) as follows.

$$\begin{aligned} &\text{Var}(\mathbb{E}[\hat{d}_1 - \hat{d}_e | d_{12}, d_{1e}, d_{2e}]) \\ &= \text{Var} \left( d_{12} \mathbb{E} \left[ 1 - \sqrt{[1 + \kappa]^+} | d_{12}, d_{1e}, d_{2e} \right] \right) \end{aligned} \quad (63)$$

$$\leq \mathbb{E} \left[ d_{12}^2 (\mathbb{E}[|x| | d_{12}, d_{1e}, d_{2e}])^2 \right] \quad (64)$$

$$\begin{aligned} &\leq \mathbb{E} \left[ \frac{1}{d_{12}^2} \mathbb{E} [ 2(d_{1e} + d_{2e})(|w_{1e}| + |w_{2e}|) + w_{1e}^2 + w_{2e}^2 \right. \\ &\quad \left. + 2d_{1e}d_{2e}|w_{\phi_e}| + 2|w_{1e}w_{2e}| |d_{12}, d_{1e}, d_{2e}|^2 \right] \\ &= \mathbb{E} \left[ \frac{\rho_e^2}{Pd_{12}^2} \left( 2(d_{1e} + d_{2e}) \frac{\sqrt{\gamma(d_{1e})} + \sqrt{\gamma(d_{2e})}}{\sqrt{\rho_e}} \right. \right. \\ &\quad \left. \left. + 2d_{1e}d_{2e}\gamma_{\phi}(d_{1e}, d_{2e}) \right. \right. \\ &\quad \left. \left. + \frac{\gamma(d_{1e}) + \gamma(d_{2e})}{\sqrt{P}} + 2 \frac{\sqrt{\gamma(d_{1e}) + \gamma(d_{2e})}}{\sqrt{P\rho_e}} \right)^2 \right] \quad (65) \\ &= \mathbb{E} \left[ \frac{\rho_e^2}{Pd_{12}^2} \left( \frac{4(d_{1e} + d_{2e})^2}{\rho_e} (\sqrt{\gamma(d_{1e})} + \sqrt{\gamma(d_{2e})})^2 \right. \right. \\ &\quad \left. \left. + 4(d_{1e}d_{2e}\gamma_{\phi}(d_{1e}, d_{2e}))^2 \right. \right. \\ &\quad \left. \left. + \frac{8(d_{1e} + d_{2e})d_{1e}d_{2e}}{\rho_e} (\sqrt{\gamma(d_{1e})} \right. \right. \\ &\quad \left. \left. + \sqrt{\gamma(d_{2e})}) \sqrt{\gamma_{\phi}(d_{1e}, d_{2e})} \right) \right] + o(1/P). \quad (66) \end{aligned}$$

where (63) follows from the fact that  $\hat{d}_e = d_{12} \sqrt{[1 + \kappa]^+}$ , and (64) follows from Lemma 3. Finally, we obtain

$$RU \leq h(\hat{d}_1 - \hat{d}_e) - h(\hat{d}_1 - d_{12} | d_{12}) \quad (67)$$

$$\leq \frac{1}{2} \log \left( 2\pi \text{Var}(\hat{d}_1 - \hat{d}_e) \right) - h(w_1 | d_{12}) \quad (68)$$



$$\begin{aligned}
&= \frac{1}{2} \log \left\{ 2\pi \mathbb{E} \left[ \frac{\rho_e}{d_{12}^2 P} \left( \frac{d_{12}^2 \rho_1}{\rho_e} \gamma(d_{12}) \right. \right. \right. \\
&\quad + 4(d_{1e} + d_{2e})^2 (\sqrt{\gamma(d_{1e})} + \sqrt{\gamma(d_{2e})})^2 \\
&\quad + (4d_{1e}d_{2e} + 64(d_{1e}d_{2e})^2) \gamma_\phi(d_{1e}, d_{2e}) \\
&\quad + 8(d_{1e} + d_{2e})d_{1e}d_{2e} (\sqrt{\gamma(d_{1e})} \\
&\quad + \sqrt{\gamma(d_{2e})}) \sqrt{\gamma_\phi(d_{1e}, d_{2e})} \\
&\quad \left. \left. \left. + 64(d_{1e} + d_{2e})^2 (\gamma(d_{1e}) + \gamma(d_{2e})) \right) \right] + o\left(\frac{1}{P}\right) \right\} \\
&\quad - \frac{1}{2} \mathbb{E} \left[ \log \left( \frac{2\pi \rho_1 \gamma(d_{12})}{P} \right) \right], \tag{69}
\end{aligned}$$

where (67) follows from (51) and (53), (68) follows from the fact that entropy of  $\hat{d}_1 - \hat{d}_e$  is upper bounded by the entropy of a Gaussian random variable that has the same variance as  $\hat{d}_1 - \hat{d}_e$ . The first term of (69) is obtained by combining (56), (62) and (66), and the second term of (69) follows from (52). Note that as  $P \rightarrow \infty$ , the  $P$  terms in (69) cancel each other since for any random variables  $u$  and  $v$ ,

$$\lim_{P \rightarrow \infty} \log \mathbb{E} \left[ \frac{u}{P} + o\left(\frac{1}{P}\right) \right] - \mathbb{E} \left[ \log \frac{v}{P} \right] = \log \mathbb{E}[u] - \mathbb{E}[\log v]$$

hence  $\lim_{P \rightarrow \infty} R_U < \infty$ .

### B. Proof of Theorem 3

When the eavesdropper does not observe the angle,  $\hat{\phi}_e = \emptyset$ . Hence

$$R_L = \lim_{n \rightarrow \infty} \frac{1}{n} \left( h(\hat{\mathbf{d}}_1 | \hat{\mathbf{d}}_{1e}, \hat{\mathbf{d}}_{2e}) - h(\hat{\mathbf{d}}_1 | \hat{\mathbf{d}}_2) \right) \tag{70}$$

First, we show that the first term in (70) is finite.

$$\begin{aligned}
&\lim_{P, n \rightarrow \infty} \frac{1}{n} h(\hat{\mathbf{d}}_1 | \hat{\mathbf{d}}_{1e}, \hat{\mathbf{d}}_{2e}) = \lim_{n \rightarrow \infty} \frac{1}{n} h(\mathbf{d}_{12} | \mathbf{d}_{1e}, \mathbf{d}_{2e}) \\
&= \lim_{n \rightarrow \infty} \frac{1}{n} \sum_{i=1}^n h(d_{12}[i] | \mathbf{d}_{1e}, \mathbf{d}_{2e}, \{d_{12}[j]\}_{j=1}^{i-1}) \\
&= \lim_{n \rightarrow \infty} \frac{1}{n} \sum_{i=1}^n h(d_{12}[i] | \mathbf{d}_{1e}, \mathbf{d}_{2e}, \{\phi_e[j]\}_{j=1}^{i-1}) \tag{71}
\end{aligned}$$

$$\begin{aligned}
&= \lim_{n \rightarrow \infty} \frac{1}{n} \sum_{i=1}^n h \left( (d_{1e}[i]^2 + d_{2e}[i]^2 - \right. \\
&\quad \left. 2d_{1e}[i]d_{2e}[i] \cos(\phi_e[i]))^{0.5} | \mathbf{d}_{1e}, \mathbf{d}_{2e}, \{\phi_e[j]\}_{j=1}^{i-1} \right) \tag{72} \\
&> -\infty \tag{73}
\end{aligned}$$

where (71) follows from the fact that a triangle is completely characterized by either three sides  $(d_{12}[i], d_{1e}[i], d_{2e}[i])$ , or two sides and an angle  $(d_{12}[i], d_{1e}[i], \phi_e[i])$ . Equation (72) follows from the cosine law. Since the probability density function of  $\phi_e$ ,  $\mathbf{d}_{12}$  and  $\mathbf{d}_{1e}, \mathbf{d}_{2e}$  are well defined, we can see that  $h(\phi_e[i] | \mathbf{d}_{1e}, \mathbf{d}_{2e}, \{\phi_e[j]\}_{j=1}^{i-1}) > -\infty$ , hence (73) holds. The second term

$$\frac{1}{n} h(\hat{\mathbf{d}}_1 | \hat{\mathbf{d}}_2) \leq \frac{1}{n} h(\hat{\mathbf{d}}_1 - \hat{\mathbf{d}}_2) \tag{74}$$

$$\begin{aligned}
&= h(w_1 - w_2) \\
&\leq \frac{1}{2} \log \left( 2\pi \mathbb{E} \left[ \frac{4\rho_{\max} \gamma(d_{12})}{P} \right] \right) \tag{75}
\end{aligned}$$

$$= \frac{1}{2} \log (2\pi \mathbb{E} [4\rho_{\max} \gamma(d_{12})]) - \frac{1}{2} \log(P).$$

where (74) follows due to the fact that conditioning reduces entropy, (75) follows from the fact  $\hat{d}_1[i] - \hat{d}_2[i] = w_1[i] - w_2[i]$  for any  $i$ . Dropping the index  $i$ , we can see that  $h(w_1 - w_2)$  is upper bounded by entropy of a Gaussian random variable that has the same variance as  $w_1 - w_2$ , which is

$$\begin{aligned}
\text{Var}(w_1 - w_2) &= \text{Var}(\mathbb{E}[w_1 - w_2]) + \mathbb{E}(\text{Var}[w_1 - w_2]) \\
&= \mathbb{E}_{d_{12}}(\text{Var}[w_1 - w_2]) \\
&\leq \mathbb{E} \left[ \frac{4\rho_{\max} \gamma(d_{12})}{P} \right].
\end{aligned}$$

Therefore, we can see that

$$\lim_{P \rightarrow \infty} \frac{R_L}{\frac{1}{2} \log(P)} \geq 1.$$

Now, we find an upper bound on  $R_U$ . Note that

$$\begin{aligned}
R_U &= \lim_{n \rightarrow \infty} \frac{1}{n} I(\hat{\mathbf{d}}_1; \hat{\mathbf{d}}_2 | \hat{\mathbf{d}}_{1e}, \hat{\mathbf{d}}_{2e}) \\
&\leq \lim_{n \rightarrow \infty} \frac{1}{n} (h(\hat{\mathbf{d}}_1 | \hat{\mathbf{d}}_{1e}, \hat{\mathbf{d}}_{2e}) - h(\hat{\mathbf{d}}_1 | \mathbf{d}_{12})) \tag{76}
\end{aligned}$$

where the first term of (76) is finite. The second term can be upper bounded as

$$\begin{aligned}
\frac{1}{n} h(\hat{\mathbf{d}}_1 | \mathbf{d}_{12}) &= h(w_1 | d_{12}) \\
&\geq \mathbb{E} \left[ \frac{1}{2} \log \left( \frac{2\pi \rho_1 \gamma(d_{12})}{P} \right) \right] \\
&= \frac{1}{2} \mathbb{E} [\log (2\pi \rho_1 \gamma(d_{12}))] - \frac{1}{2} \log(P),
\end{aligned}$$

therefore

$$\lim_{P \rightarrow \infty} \frac{R_U}{\frac{1}{2} \log(P)} \leq 1.$$

Since  $R_L \leq R_U$  by definition, the proof is complete.

## APPENDIX D ON OBSERVATION BIAS

Nodes' observations may have bias due to several factors. We consider two different source of bias; clock mismatch and multipath fading. We will see that different types of bias may have different outcomes. In this part, we present our results for no GLI. However, the conclusions are valid for perfect GLI as well.

### A. Clock Mismatch

Assume that there is a clock mismatch between nodes 1, and 2. Consequently, all the observations of  $d_{12}$  of nodes 1 and 2 in localization phase are shifted by a random value  $\eta_1$  and  $\eta_2$  respectively:

$$\hat{d}_j[i] = d_{12}[i] + w_j[i] + \eta_j \tag{77}$$

for  $j \in \{1, 2\}$ , where  $w_j[i]$  is as given in (20). We assume the amount of clock mismatch is a non-random, but unknown parameter, which remains constant throughout the entire session<sup>12</sup>.

<sup>12</sup>The underlying assumption is that, the clock mismatch variations are much slower than the duration of the key-generation sessions

Since  $w_j[i]$ ,  $j \in \{1, 2\}$  are zero mean random variables,

$$\mathbb{E}[\hat{d}_j[i]|\eta_1, \eta_2] = \mathbb{E}[d_{12}[i]] + \eta_j. \quad (78)$$

Hence, with the knowledge of the statistics of the mobility, each node  $j \in \{1, 2\}$  can obtain a perfect estimate of the amount of clock mismatch  $\eta_j$  as  $n \rightarrow \infty$ , by simply calculating the difference between the long-term average of the distance observations  $\hat{d}_j[i]$  for all  $i$  and the known mean distance  $\mathbb{E}[d_{12}]$ . Then this value can be broadcast in the public discussion phase. Therefore, clock mismatch does not affect the theoretical bounds of secret key generation rates.

### B. Multipath Fading

There may be a bias in the observations when the nodes experience multipath fading. An example of this is time of arrival observation of distances when the nodes are not within their line of sight. Note that, this kind of bias does not remain constant, and varies from one slot to the other. The impact of fading can be viewed as that of an additional observation noise source and the distance observations can be written as

$$\hat{d}_j[i] = d_{12}[i] + w_j[i] + \eta_j[i]$$

for  $j \in \{1, 2\}$ .

Consequently, one will observe a reduction in the key rate. For example, with no angle observation at the eavesdropper, we know from Section V-A that the key rate grows unboundedly with the beacon power  $P$ . However, with multipath fading, independent over different locations,

$$\begin{aligned} \lim_{P \rightarrow \infty} h(\hat{\mathbf{d}}_1|\hat{\mathbf{d}}_2) &= h(\boldsymbol{\eta}_1|\boldsymbol{\eta}_2) \\ &\stackrel{(a)}{=} h(\boldsymbol{\eta}_1) > -\infty, \end{aligned}$$

where  $\boldsymbol{\eta}_1 = \{\eta_1[i]\}_{i=1}^n$ , and (a) follows since  $\boldsymbol{\eta}_1$  and  $\boldsymbol{\eta}_2$  are independent. Hence, following an identical approach to Section V-A, one see that  $\lim_{P \rightarrow \infty} R_L < \infty$ , i.e., the secret key rate remains bounded even as the power grows unboundedly.

### REFERENCES

- [1] U. M. Maurer, "Secret key agreement by public discussion from common information," *IEEE Trans. Information Theory*, vol.39, no.3, pp.733-742, May 1993
- [2] R. Ahlswede and I. Csiszar, "Common randomness in information theory and cryptography. I. Secret sharing," *IEEE Trans. Information Theory*, vol.39, no.4, pp.1121-1132, Jul 1993
- [3] U. M. Maurer and S. Wolf, "Unconditionally secure key agreement and the intrinsic conditional information," *IEEE Trans. Information Theory*, vol.45, no.2, pp.499-514, Mar 1999
- [4] I. Csiszar and P. Narayan, "Secrecy capacities for multiterminal channel models," *IEEE Trans. Information Theory*, vol.54, no.6, pp.2437-2452, June 2008
- [5] U. M. Maurer and S. Wolf, "Secret-key agreement over unauthenticated public channels .I. Definitions and a completeness result," *IEEE Transactions on Information Theory*, vol.49, no.4, pp. 822- 831, April 2003
- [6] I. Csiszar and P. Narayan, "Common randomness and secret key generation with a helper," *IEEE Transactions on Information Theory*, vol.46, no.2, pp.344-366, Mar 2000
- [7] U. M. Maurer, and S. Wolf, "Information-theoretic key agreement: From weak to strong secrecy for free," *Advances in CryptologyEUROCRYPT 2000*, Springer Berlin Heidelberg, 2000.
- [8] S. Gezici, Z. Tian, G. B. Giannakis, H. Kobayashi, A.F. Molisch, H.V. Poor, and Z. Sahinoglu, "Localization via ultra-wideband radios: a look at positioning aspects for future sensor networks," *IEEE Signal Processing Magazine*, vol.22, no.4, pp. 70- 84, July 2005
- [9] Y. Shen and M.Z. Win, "Fundamental limits of wideband localization Part I: A general framework," *IEEE Trans. Information Theory*, vol.56, no.10, pp.4956-4980, Oct. 2010
- [10] H. Buhman, N. Chandran, V. Goyal, R. Ostrovsky and C. Schaffner, "Position-based quantum cryptography: Impossibility and constructions," 2010
- [11] A. Srivinasan and J. Vu, "A survey on secure localization in wireless sensor networks", *Encyclopedia of Wireless and Mobile Communications*, 2007
- [12] R. Poovendran, C. Wang, S. Roy, "Secure localization and time synchronization for wireless sensor and ad-hoc networks", Springer Verlag, 2007
- [13] N. Chandran, V. Goyal, R. Moriarty and R. Ostrovsky, "Position based cryptography," *Cryptology ePrint Archive*, 2009, <http://eprint.iacr.org/2009/>
- [14] Wilson, R.; Tse, D.; Scholtz, R.A.; , "Channel identification: Secret sharing using reciprocity in ultrawideband channels," *IEEE International Conf. Ultra-Wideband, ICUWB 2007*, pp.270-275, 24-26 Sept. 2007
- [15] Kirchner, Nathan, and Tomonari Furukawa, "Infrared localisation for indoor uavs," *ICST05: Proceedings of the 2005 International Conference on Sensing Technology*, 2005.
- [16] Jimnez, A. R., and F. Seco, "Ultrasonic Localization Methods for Accurate Positioning," Instituto de Automatica Industrial, Madrid (2005).
- [17] S. Verdú and T. S. Han, "A general formula for channel capacity," *IEEE Transactions on Information Theory*, vol.40, no.4, pp.1147-1157, Jul 1994
- [18] M. R. Bloch and J. N. Laneman, "Secrecy from resolvability," *arXiv:1105.5419v1 [cs.IT]*, May 2011
- [19] D. Jourdan, D. Dardari and M. Win, "Position error bound for UWB localization in dense cluttered environments," *IEEE Transactions on Aerospace and Electronic Systems*, vol.44, no.2, pp.613-628, April 2008
- [20] S. Mathur, W. Trappe, N. Mandayam, C. Ye and A. Reznik, "Radio-telepathy: extracting a secret key from an unauthenticated wireless channel," *Proceedings of the 14th ACM international conference on Mobile computing and networking (MobiCom '08) ACM*, New York, NY, USA, 128-139
- [21] S. Jana, S. N. Premnath, M. Clark, S. K. Kasera, N. Patwari and S. V. Krishnamurthy, "On the effectiveness of secret key extraction from wireless signal strength in real environments," *Proceedings of the 15th annual international conference on Mobile computing and networking (MobiCom '09) ACM*, New York, NY, USA, 321-332
- [22] J. Zhang, S.K. Kasera and N. Patwari, "Mobility Assisted Secret Key Generation Using Wireless Link Signatures," *Proc. IEEE INFOCOM 2010*, vol., no., pp.1-5, 14-19 March 2010
- [23] N. Patwari, J. Croft, S. Jana and S. K. Kasera, "High-Rate Uncorrelated Bit Extraction for Shared Secret Key Generation from Channel Measurements," *IEEE Transactions on Mobile Computing*, vol.9, no.1, pp.17-30, Jan. 2010
- [24] C. Ye, S. Mathur, A. Reznik, Y. Shah, W. Trappe, and N. B. Mandayam, "Information-theoretically secret key generation for fading wireless channels," *IEEE Transactions on Information Forensics and Security*, no. 2 (2010): 240-254.
- [25] S. Banerjee and A. Mishra, "Secure spaces: Location-based secure group communication for wireless networks," *ACM MobiCom*, vol. 7, pp. 68 70, Sep. 2002.
- [26] S. Mathur, R. Miller, A. Varshavsky, W. Trappe, and N. Mandayam, "Proximate: Proximity-based secure pairing using ambient wireless signals," *ACM MobiSys*, pp. 211224, Jun. 2011.
- [27] NIST, "A statistical test suite for the validation of random number generators and pseudo random number generators for cryptographic applications," 2001
- [28] G.Brassard and L. Salvail, "Secret-key reconciliation by public discussion," in *Workshop on the theory and application of cryptographic techniques on Advances in cryptology (EUROCRYPT '93)*, Tor Hellesteth (Ed.). Springer-Verlag New York, Inc., Secaucus, NJ, USA, 410-423.
- [29] <https://code.google.com/p/miniz/>
- [30] O. S. Oguejiofor, V. N. Okorogu and OBO Adewale Abe, "Outdoor Localization System Using RSSI Measurement of Wireless Sensor Network"
- [31] D. Klinc, H. Jeongseok, S.W. McLaughlin, J. Barros, K. Byung-Jae, "LDPC Codes for the Gaussian Wiretap Channel," *IEEE Transactions on Information Forensics and Security*, vol.6, no.3, pp.532,540, Sept. 2011